

ON NONLOCAL PROBLEMS WITH INHOMOGENEOUS LOCAL BOUNDARY CONDITIONS

BURAK AKSOYLU AND GEORGE A. GAZONAS

*CCDC Army Research Laboratory, Attn:FCDD-RLW-MB,
Aberdeen Proving Ground, MD 21005, USA &
Wayne State University, Department of Mathematics, Detroit, MI 48202, USA.*

*CCDC Army Research Laboratory, Attn:FCDD-RLW-MB,
Aberdeen Proving Ground, MD 21005, USA.*

ABSTRACT. This work aims to provide a comprehensive treatment on how to enforce inhomogeneous local boundary conditions (BC) in nonlocal problems in 1D. In prior work, we have presented novel governing operators with homogeneous BC. Here, we extend the construction to inhomogeneous BC. The construction of the operators is inspired by peridynamics. The operators agree with the original peridynamic operator in the bulk of the domain and simultaneously enforce local Dirichlet or Neumann BC.

We explain methodically how to construct forcing functions to enforce local BC and their relationship to initial values. We present exact solutions with both homogeneous and inhomogeneous BC and utilize the resulting error to verify numerical experiments. We explain the critical role of the Hilbert-Schmidt property in enforcing local BC rigorously. For the Neumann BC, we prescribe an interpolation strategy to find the appropriate value of the forcing function from its derivative. We also present numerical experiments with unknown solution and report the computed displacement and strain fields.

Keywords: Nonlocal Wave Equation, Nonlocal Operator, Inhomogeneous Local Boundary Condition, Peridynamics, Functional Calculus.

Mathematics Subject Classification (2000): 65R20, 65M70, 47G10, 74B99.

1. INTRODUCTION

We consider the following nonlocal wave equations with inhomogeneous local Dirichlet and local Neumann boundary conditions (BC), respectively:

$$u_{tt}^{\mathbb{D}}(x, t) + \mathcal{M}_{\mathbb{D}} u^{\mathbb{D}}(x, t) = b^{\mathbb{D}}(x, t), \quad (x, t) \in \Omega \times (0, T), \quad (1.1a)$$

$$u^{\mathbb{D}}(\pm 1, t) = \alpha_{\pm}^{\mathbb{D}}(t), \quad (1.1b)$$

$$u^{\mathbb{D}}(x, 0) = \phi_{\mathbb{D}}(x), \quad (1.1c)$$

$$u_t^{\mathbb{D}}(x, 0) = \psi_{\mathbb{D}}(x), \quad (1.1d)$$

E-mail address: burak@wayne.edu, george.a.gazonas.civ@mail.mil.

Date: June 16, 2019.

$$u_{tt}^{\mathbb{N}}(x, t) + \mathcal{M}_{\mathbb{N}} u^{\mathbb{N}}(x, t) = b^{\mathbb{N}}(x, t), \quad (x, t) \in \Omega \times (0, T), \quad (1.2a)$$

$$u_x^{\mathbb{N}}(\pm 1, t) = \alpha_{\pm}^{\mathbb{N}}(t), \quad (1.2b)$$

$$u^{\mathbb{N}}(x, 0) = \phi_{\mathbb{N}}(x), \quad (1.2c)$$

$$u_t^{\mathbb{N}}(x, 0) = \psi_{\mathbb{N}}(x), \quad (1.2d)$$

on the domain $\Omega := (-1, 1)$ for some $T > 0$ where the variable u^{BC} represents the displacement. The problems (1.1) and (1.2) fall into the class of initial boundary value problems. We have studied the above nonlocal wave equations with homogeneous local BC in prior work [1, 2, 6]. We extended the treatment to inhomogeneous BC in a preliminary study [7]. The primary purpose of this study is to present a comprehensive treatment.

The main theoretical contributions in this study are:

- (1) We present exact solutions and utilize the resulting error to verify numerical experiments.
- (2) We explain the critical role of Hilbert-Schmidt property in satisfying BC rigorously.
- (3) We provide the relationships between forcing function, boundary condition, and initial values used to enforce local BC.
- (4) For the Neumann BC, we prescribe an interpolation strategy to find the appropriate value of the forcing function from its derivative.

To the authors' knowledge, our operators are the first nonlocal operators that can enforce local displacement and strain BC. When extended to vector valued problems, they will help apply peridynamics to problems that require local BC. The operators are inspired by the theory of peridynamics, a nonlocal formulation of continuum mechanics developed by Silling [17]. They agree with the original peridynamic operator in the bulk of the domain and simultaneously enforce local BC.

We studied various aspects of local BC in nonlocal problems [1, 2, 3, 4, 5, 6, 8, 10]. Building on [10], we generalized the results in \mathbb{R} to a bounded domain [1, 2], a critical feature for all practical applications. In [2], we laid the theoretical foundations and in [1], we applied the foundations to numerically solve wave propagation problems using local BC. In [4], we constructed the first 1D operators that agree with the original bond-based peridynamic operator in the bulk of the domain and simultaneously enforce local Neumann or Dirichlet BC which we denote by $\mathcal{M}_{\mathbb{N}}$ and $\mathcal{M}_{\mathbb{D}}$, respectively. We carried out numerical experiments by utilizing $\mathcal{M}_{\mathbb{N}}$ and $\mathcal{M}_{\mathbb{D}}$ as governing operators in [1]. We extended the operators to higher dimensions in [6]. In [5], we methodically apply functional calculus to general nonlocal problems. In [8], we study the conditioning of nonlocal operators together with error analysis.

Our approach is not limited to peridynamics, the abstractness of the theoretical methods used allows generalization to other nonlocal theories. Our approach presents a unique way of combining the powers of abstract operator theory with numerical computing [1]. Nonlocal modeling is an emerging field. See the relevant review and news articles [12, 13, 14, 18] for a comprehensive discussion, and the book [16].

The rest of the paper is structured as follows. In Sec. 2, we outline the key steps to construct the nonlocal operators using functional calculus. In Sec. 3, we present the main construction for boundary value problems by providing the relationships between forcing function, BC, and initial values. In Sec. 4, we explain how the Hilbert-Schmidt property gives rise to uniform convergence, which in turn is used to satisfy BC rigorously. The series solutions from the classical theory cannot guarantee such rigor, and hence, qualify only as formal solutions. In Sec. 5, we present exact

solutions with homogeneous BC. In Sec. 6, we present exact solutions with inhomogeneous BC using the method of shifting the data. In Sec. 7, we set the stage for numerical experiments by choosing kernel functions. We introduce the appropriate scaling so that the discretized nonlocal operator captures the discretized Laplace operator when $\delta = h$. The discretized nonlocal operator enjoys the zero row sum property which can be spoiled due round-off for small δ . We carefully explain how to avoid it. Enforcing the Neumann BC involves taking the spatial derivative of the forcing function. However, the forcing function itself is present in the governing equation. In Sec. 8, we prescribe an interpolation strategy to find the appropriate value of the forcing function from its derivative. In Sec. 9, we present the implementation and the numerical experiments. Finally, we conclude in Sec. 10.

2. THE CONVOLUTION AND THE GOVERNING OPERATORS

In this section, we explain the key steps in construction of the governing operator \mathcal{M}_{BC} . We observe that the peridynamic governing operator contains a convolution operator. First, we construct the convolution operators $\mathcal{C}_{\mathbf{a}}$ and $\mathcal{C}_{\mathbf{p}}$ with antiperiodic and periodic BC, respectively, using the eigenfunctions

$$e_k^{\mathbf{a}}(x) := \frac{1}{\sqrt{2}} e^{i\pi(k+\frac{1}{2})x}, \quad k \in \mathbb{N}, \quad \text{and} \quad e_k^{\mathbf{p}}(x) := \frac{1}{\sqrt{2}} e^{i\pi kx}, \quad k \in \mathbb{N},$$

of the classical operator $A_{\mathbf{a}}$ and $A_{\mathbf{p}}$ in which the BC information is already encoded. For a given kernel function $C \in L^2(\Omega)$, the convolution operator, for $u \in L^2(\Omega)$, is defined as

$$\mathcal{C}_{\text{BC}}u(x) := \sqrt{2} \sum_{k \in \mathbb{N}} \langle e_k^{\text{BC}} | C \rangle \langle e_k^{\text{BC}} | u \rangle e_k^{\text{BC}}(x), \quad \text{BC} \in \{\mathbf{a}, \mathbf{p}\},$$

where $\langle \cdot | \cdot \rangle$ denotes the $L^2(\Omega)$ inner product. We define $\mathbb{N}_{\text{D}} := \mathbb{N} \setminus \{0\}$ and $\mathbb{N}_{\text{N}} := \mathbb{N}$. The operators \mathcal{C}_{BC} turn out to be bounded functions of the classical operator A_{BC} , thereby maintaining the connection to A_{BC} .

In this study, we consider only the operators \mathcal{M}_{D} and \mathcal{M}_{N} where D and N denote the Dirichlet and Neumann BC. Hence, in the rest of the discussion, we set $\text{BC} \in \{\text{D}, \text{N}\}$. The operator \mathcal{M}_{BC} is constructed using *functional calculus* on the classical self-adjoint operator A_{BC} . We are in search of a suitable regulating function $f_{\text{BC}} : \sigma(A_{\text{BC}}) \rightarrow \mathbb{R}$ that would connect the nonlocal operator \mathcal{M}_{BC} to A_{BC} , i.e., $\mathcal{M}_{\text{BC}} = f_{\text{BC}}(A_{\text{BC}})$. This regulating function should be bounded so that the end product \mathcal{M}_{BC} is a bounded operator. Eventually, we end up with the nonlocal governing operator \mathcal{M}_{BC} that is densely defined in $L^2(\Omega)$ with a domain that encodes the prescribed BC, bounded, and self-adjoint. Therefore, the operator \mathcal{M}_{BC} has a unique bounded extension to $L^2(\Omega)$. Consequently, we find that a construction involving densely defined operators provides a suitable framework for treating local BC in the nonlocal wave equation.

In this work, the choice of f_{BC} is inspired by the theory of peridynamics. In prior work, we discovered that the peridynamic governing operator for the case $\Omega = \mathbb{R}$ is a function of the classical operator [10]. We reuse that regulating function for the case of $\Omega = (-1, 1)$. Our choice of regulating functions is

$$f_{\text{BC}} : \sigma(A_{\text{BC}}) \rightarrow \mathbb{R}, \quad f_{\text{BC}}(\lambda_k^{\text{BC}}) = \langle 1 | C \rangle - \sqrt{2} \begin{cases} \langle e_{k/2}^{\mathbf{p}} | C \rangle & \text{if } k \in \mathbb{N}_{\text{BC}} \text{ is even,} \\ \langle e_{(k-1)/2}^{\mathbf{a}} | C \rangle & \text{if } k \in \mathbb{N}_{\text{BC}} \text{ is odd.} \end{cases}$$

Utilizing the convolution operators \mathcal{C}_a and \mathcal{C}_p obtained by functional calculus on A_a and A_p , respectively, defining $c := \langle 1|C \rangle$, we proved in [1, 4] that

$$\begin{aligned} f_D(A_D)u^D &= (c - \mathcal{C}_a P_e - \mathcal{C}_p P_o)u^D = \mathcal{M}_D u^D, \\ f_N(A_N)u^N &= (c - \mathcal{C}_p P_e - \mathcal{C}_a P_o)u^N = \mathcal{M}_N u^N, \end{aligned}$$

where we denote the orthogonal projections that give the even and odd parts, respectively, by $P_e, P_o : L^2(\Omega) \rightarrow L^2(\Omega)$, whose definitions are

$$P_e u(x) := \frac{u(x) + u(-x)}{2}, \quad P_o u(x) := \frac{u(x) - u(-x)}{2}.$$

The crucial step in the construction of \mathcal{M}_{BC} is the application of the spectral theorem for bounded operators. Namely, for $u^{BC} = \sum_k \langle e_k^{BC} | u^{BC} \rangle e_k^{BC}$, we have

$$\mathcal{M}_{BC} u^{BC} = f_{BC}(A_{BC})u^{BC} = \sum_{k \in \mathbb{N}_{BC}} f_{BC}(\lambda_k^{BC}) \langle e_k^{BC} | u^{BC} \rangle e_k^{BC}. \quad (2.1)$$

For an extended discussion on the treatment of general nonlocal problems using functional calculus, see [5].

An integral representation of the series (2.1) is more convenient for implementation. We gave such representations in [1] and the governing operators take the form

$$\begin{aligned} (\mathcal{M}_{BC} - c)u^{BC}(x, t) &= - \int_{\Omega} K_{BC}(x, x')u^{BC}(x', t) dx', \\ K_D(x, x') &:= \frac{1}{2} \{ [\widehat{C}_a(x' - x) + \widehat{C}_a(x' + x)] + [\widehat{C}_p(x' - x) - \widehat{C}_p(x' + x)] \}, \\ K_N(x, x') &:= \frac{1}{2} \{ [\widehat{C}_p(x' - x) + \widehat{C}_p(x' + x)] + [\widehat{C}_a(x' - x) - \widehat{C}_a(x' + x)] \}, \end{aligned} \quad (2.2)$$

where we denote the periodic and antiperiodic extensions of $C(x)$ from $(-1, 1)$ to $(-2, 2)$, respectively, as follows

$$\widehat{C}_p(x) := \begin{cases} C(x+2), & x \in (-2, -1), \\ C(x), & x \in (-1, 1), \\ C(x-2), & x \in (1, 2), \end{cases} \quad \widehat{C}_a(x) := \begin{cases} -C(x+2), & x \in (-2, -1), \\ C(x), & x \in (-1, 1), \\ -C(x-2), & x \in (1, 2). \end{cases}$$

In (2.2), the constant $c := \int_{\Omega} C(x) dx$ and the kernel function K_{BC} correspond to the stiffness density and the density of stiffness density, respectively. In addition, u_x^N represents strain.

3. FORCING FUNCTION, BC, AND INITIAL VALUE RELATIONSHIPS

In order to find the suitable forcing function that enforces the prescribed BC, we need to identify the governing ordinary differential equation (ODE) on the boundary. For this identification, we assume that $u^D \in \mathcal{C}^2(\overline{\Omega} \times [0, T])$, $u^N \in \mathcal{C}^3(\overline{\Omega} \times [0, T])$, and $b^D \in \mathcal{C}^0(\overline{\Omega} \times [0, T])$, $b^N \in \mathcal{C}^1(\overline{\Omega} \times [0, T])$. Let us explain a crucial point in the choice of these subspaces and elaborate on the subspace of u^D only. The case of Neumann BC easily follows. In fact, the solution $u^D(\cdot, t)$ belongs to $L^2(\Omega)$ for any $t \in [0, T]$. But, $L^2(\Omega)$ ignores the values of $u(\cdot, t)$ on the boundary of Ω . In order to determine the boundary behavior of $u(\cdot, t)$, we visualize it as a limit of a sequence from $\mathcal{C}^2(\overline{\Omega})$, a space that is aware of the function values on the boundary of Ω . We accomplish this by the density of $\mathcal{C}^2(\overline{\Omega})$ in $L^2(\Omega)$. Note that this density is in alignment with \mathcal{M}_D 's property of being densely defined. So, when we write u^D , we implicitly mean a sequence $u_n^D(\cdot, t) \in \mathcal{C}^2(\overline{\Omega})$ approaching $u^D(\cdot, t)$, i.e.,

$\lim_{n \rightarrow \infty} u_n^{\text{D}}(\cdot, t) = u^{\text{D}}(\cdot, t)$ in the $L^2(\Omega)$ -norm. In this section, with a slight abuse of notation, we prefer to use $u^{\text{D}}(\cdot, t)$ instead of $u_n^{\text{D}}(\cdot, t)$. The action of \mathcal{M}_{D} on $u^{\text{D}}(\cdot, t)$ is seen as

$$\begin{aligned} \mathcal{M}_{\text{D}} u^{\text{D}}(\cdot, t) &= \mathcal{M}_{\text{D}} \lim_{n \rightarrow \infty} u_n^{\text{D}}(\cdot, t) \\ &= \lim_{n \rightarrow \infty} \mathcal{M}_{\text{D}} u_n^{\text{D}}(\cdot, t) \quad \text{using the boundedness of } \mathcal{M}_{\text{D}}. \end{aligned}$$

For more rigorous discussion of the function spaces, see [7, Sec. 1].

We emphasize that our construction does not assume any smoothness on the initial displacement and initial velocity. We can treat

$$u^{\text{BC}}(x, 0), u_t^{\text{BC}}(x, 0) \in L^2(\Omega). \quad (3.1)$$

We have substantiated the validity of assumption (3.1) by choosing discontinuous initial displacement profiles for numerical experiments in 1D [1] as well as in 2D [6]. The construction only assumes the existence of the following limits

$$\lim_{x \rightarrow \pm 1} u^{\text{D}}(x, t), \lim_{x \rightarrow \pm 1} u_x^{\text{N}}(x, t), \text{ and } \lim_{x \rightarrow \pm 1} u_t^{\text{BC}}(x, t),$$

and they should be provided as boundary data to set up the problem.

On the boundary, denote the displacement, the strain and the forcing functions by

$$\begin{aligned} u_{\pm}^{\text{D}}(t) &:= \lim_{x \rightarrow \pm 1} u^{\text{D}}(x, t) \quad \text{and} \quad b_{\pm}^{\text{D}}(t) := \lim_{x \rightarrow \pm 1} b^{\text{D}}(x, t), \\ u_{x, \pm}^{\text{N}}(t) &:= \lim_{x \rightarrow \pm 1} \frac{\partial u^{\text{N}}}{\partial x}(x, t) \quad \text{and} \quad b_{x, \pm}^{\text{N}}(t) := \lim_{x \rightarrow \pm 1} \frac{\partial b^{\text{N}}}{\partial x}(x, t). \end{aligned}$$

In order to investigate the behavior of the solution on the boundary, first we study the action of the governing operator \mathcal{M}_{BC} on the boundary. By the Lebesgue Dominated Convergence Theorem and the design of the kernel functions $K_{\text{BC}}(x, x')$, we have

$$\begin{aligned} \lim_{x \rightarrow \pm 1} (\mathcal{M}_{\text{D}} - c) u^{\text{D}}(x, t) &= - \lim_{x \rightarrow \pm 1} \int_{\Omega} K_{\text{D}}(x, x') u^{\text{D}}(x', t) dx' \\ &= - \int_{\Omega} \lim_{x \rightarrow \pm 1} K_{\text{D}}(x, x') u^{\text{D}}(x', t) dx' = 0, \end{aligned} \quad (3.2)$$

$$\begin{aligned} \lim_{x \rightarrow \pm 1} \frac{\partial}{\partial x} (\mathcal{M}_{\text{N}} - c) u^{\text{N}}(x, t) &= - \lim_{x \rightarrow \pm 1} \frac{\partial}{\partial x} \int_{\Omega} K_{\text{N}}(x, x') u^{\text{N}}(x', t) dx' \\ &= - \int_{\Omega} \lim_{x \rightarrow \pm 1} \frac{\partial K_{\text{N}}}{\partial x}(x, x') u^{\text{N}}(x', t) dx' = 0. \end{aligned} \quad (3.3)$$

The governing equations (1.1a) and (1.2a) under the action of $\lim_{x \rightarrow \pm 1}$ and $\lim_{x \rightarrow \pm 1} \frac{\partial}{\partial x}$, respectively, reduce to the following ODE:

$$\frac{d^2 u_{\pm}^{\text{D}}}{dt^2}(t) + c u_{\pm}^{\text{D}}(t) = b_{\pm}^{\text{D}}(t), \quad t \in (0, T), \quad (3.4)$$

$$\frac{d^2 u_{x, \pm}^{\text{N}}}{dt^2}(t) + c u_{x, \pm}^{\text{N}}(t) = b_{x, \pm}^{\text{N}}(t), \quad t \in (0, T). \quad (3.5)$$

In order to obtain a unique solution to (3.4) and (3.5), we need to prescribe the two initial values $u_{\pm}^{\text{D}}(0)$ and $\frac{du_{\pm}^{\text{D}}}{dt}(0)$ and $u_{x, \pm}^{\text{N}}(0)$ and $\frac{du_{x, \pm}^{\text{N}}}{dt}(0)$, respectively.

By taking $\lim_{x \rightarrow \pm 1}$ in (1.1c) and (1.1d) and $\lim_{x \rightarrow \pm 1} \frac{\partial}{\partial x}$ in (1.2c) and (1.2d), we immediately identify the initial displacement and velocity for the Dirichlet problem and initial strain and strain rate for the Neumann problem as

$$u_{\pm}^{\mathbb{D}}(0) = \phi_{\mathbb{D}}(\pm 1) \quad \text{and} \quad \frac{du_{\pm}^{\mathbb{D}}}{dt}(0) = \psi_{\mathbb{D}}(\pm 1), \quad (3.6)$$

$$u_{x,\pm}^{\mathbb{N}}(0) = \phi'_{\mathbb{N}}(\pm 1) \quad \text{and} \quad \frac{du_{x,\pm}^{\mathbb{N}}}{dt}(0) = \psi'_{\mathbb{N}}(\pm 1). \quad (3.7)$$

Putting together (3.4) and (3.6), we arrive at the initial value problem (IVP) on the boundary for the Dirichlet problem:

$$\begin{aligned} \frac{d^2 u_{\pm}^{\mathbb{D}}}{dt^2}(t) + cu_{\pm}^{\mathbb{D}}(t) &= b_{\pm}^{\mathbb{D}}(t), \quad t \in (0, T), \\ u_{\pm}^{\mathbb{D}}(0) &= \phi_{\mathbb{D}}(\pm 1) \quad \text{and} \quad \frac{du_{\pm}^{\mathbb{D}}}{dt}(0) = \psi(\pm 1). \end{aligned} \quad (3.8)$$

Similarly, putting (3.5) and (3.7) together, we arrive at the IVP on the boundary for the Neumann problem:

$$\begin{aligned} \frac{d^2 u_{x,\pm}^{\mathbb{N}}}{dt^2}(t) + cu_{x,\pm}^{\mathbb{N}}(t) &= b_{x,\pm}^{\mathbb{N}}(t), \quad t \in (0, T), \\ u_{x,\pm}^{\mathbb{N}}(0) &= \phi'_{\mathbb{N}}(\pm 1) \quad \text{and} \quad \frac{du_{x,\pm}^{\mathbb{N}}}{dt}(0) = \psi'_{\mathbb{N}}(\pm 1). \end{aligned} \quad (3.9)$$

On the other hand, the BC (1.1b) and (1.2b) demand a solution from (3.8) and (3.9) that are equal to $\alpha_{\pm}^{\mathbb{D}}(t)$ and $\alpha_{\pm}^{\mathbb{N}}(t)$, respectively. Hence, we identify the initial displacement and velocity, for the Dirichlet problem and initial strain and initial strain rate, for the Neumann problem, as well as the corresponding forcing functions. When the following choices are made,

$$\text{Dirichlet: } b_{\pm}^{\mathbb{D}}(t) = \frac{d^2 \alpha_{\pm}^{\mathbb{D}}}{dt^2}(t) + c\alpha_{\pm}^{\mathbb{D}}(t), \quad \phi_{\mathbb{D}}(\pm 1) = \alpha_{\pm}^{\mathbb{D}}(0), \quad \psi_{\mathbb{D}}(\pm 1) = \frac{d\alpha_{\pm}^{\mathbb{D}}}{dt}(0), \quad (3.10)$$

$$\text{Neumann: } b_{x,\pm}^{\mathbb{N}}(t) = \frac{d^2 \alpha_{\pm}^{\mathbb{N}}}{dt^2}(t) + c\alpha_{\pm}^{\mathbb{N}}(t), \quad \phi'_{\mathbb{N}}(\pm 1) = \alpha_{\pm}^{\mathbb{N}}(0), \quad \psi'_{\mathbb{N}}(\pm 1) = \frac{d\alpha_{\pm}^{\mathbb{N}}}{dt}(0), \quad (3.11)$$

the IVP (3.8) for the Dirichlet problem takes the form

$$\begin{aligned} \frac{d^2 u_{\pm}^{\mathbb{D}}}{dt^2}(t) + cu_{\pm}^{\mathbb{D}}(t) &= \frac{d^2 \alpha_{\pm}^{\mathbb{D}}}{dt^2}(t) + c\alpha_{\pm}^{\mathbb{D}}(t), \quad t \in (0, T), \\ u_{\pm}^{\mathbb{D}}(0) &= \alpha_{\pm}^{\mathbb{D}}(0) \quad \text{and} \quad \frac{du_{\pm}^{\mathbb{D}}}{dt}(0) = \frac{d\alpha_{\pm}^{\mathbb{D}}}{dt}(0). \end{aligned}$$

Similarly, the IVP (3.9) for the Neumann problem takes the form

$$\begin{aligned} \frac{d^2 u_{x,\pm}^{\mathbb{N}}}{dt^2}(t) + cu_{x,\pm}^{\mathbb{N}}(t) &= \frac{d^2 \alpha_{\pm}^{\mathbb{N}}}{dt^2}(t) + c\alpha_{\pm}^{\mathbb{N}}(t), \quad t \in (0, T), \\ u_{x,\pm}^{\mathbb{N}}(0) &= \alpha_{\pm}^{\mathbb{N}}(0) \quad \text{and} \quad \frac{du_{x,\pm}^{\mathbb{N}}}{dt}(0) = \frac{d\alpha_{\pm}^{\mathbb{N}}}{dt}(0). \end{aligned}$$

Consequently, we guarantee that the solutions to (3.8) and (3.9) are exactly $\alpha_{\pm}^{\mathbb{D}}(t)$ and $\alpha_{\pm}^{\mathbb{N}}(t)$, respectively. As seen above, the way to enforce inhomogeneous local BC is by the use of a forcing function on the boundary only, *not in the interior of Ω* . This is a major difference between enforcing local and nonlocal BC.

Remark 3.1. Since $u^{\mathbb{D}} \in C^2(\overline{\Omega} \times [0, T])$, the choices (3.10)₂ and (3.10)₃ correspond to the continuity of $u^{\mathbb{D}}$ and $u_t^{\mathbb{D}}$, respectively, at the corner points $(\pm 1, 0)$. More precisely, they are implications for the following interchange of limits.

$$\begin{aligned}\phi_{\mathbb{D}}(\pm 1) &= \lim_{x \rightarrow \pm 1} \lim_{t \rightarrow 0} u^{\mathbb{D}}(x, t) = \lim_{t \rightarrow 0} \lim_{x \rightarrow \pm 1} u^{\mathbb{D}}(x, t) = \alpha_{\pm}^{\mathbb{D}}(0), \\ \psi_{\mathbb{D}}(\pm 1) &= \lim_{x \rightarrow \pm 1} \lim_{t \rightarrow 0} u_t^{\mathbb{D}}(x, t) = \lim_{t \rightarrow 0} \lim_{x \rightarrow \pm 1} u_t^{\mathbb{D}}(x, t) = \frac{d\alpha_{\pm}^{\mathbb{D}}}{dt}(0).\end{aligned}$$

Similarly, since $u^{\mathbb{N}} \in C^3(\overline{\Omega} \times [0, T])$, the choices (3.11)₂ and (3.11)₃ correspond to the continuity of $u_x^{\mathbb{N}}$ and $u_{xt}^{\mathbb{N}}$, respectively, at the corner points $(\pm 1, 0)$.

$$\begin{aligned}\phi'_{\mathbb{N}}(\pm 1) &= \lim_{x \rightarrow \pm 1} \lim_{t \rightarrow 0} \frac{\partial u^{\mathbb{N}}}{\partial x}(x, t) = \lim_{t \rightarrow 0} \lim_{x \rightarrow \pm 1} \frac{\partial u^{\mathbb{N}}}{\partial x}(x, t) = \alpha_{\pm}^{\mathbb{N}}(0), \\ \psi'_{\mathbb{N}}(\pm 1) &= \lim_{x \rightarrow \pm 1} \lim_{t \rightarrow 0} \frac{\partial u_t^{\mathbb{N}}}{\partial x}(x, t) = \lim_{t \rightarrow 0} \lim_{x \rightarrow \pm 1} \frac{\partial u_t^{\mathbb{N}}}{\partial x}(x, t) = \frac{d\alpha_{\pm}^{\mathbb{N}}}{dt}(0).\end{aligned}$$

4. THE HILBERT-SCHMIDT PROPERTY AND THE GOVERNING OPERATOR

Resorting to the integral representation of the operators, since $K_{\text{BC}}(x, x') \in L^2(\Omega \times \Omega)$, we see that the operator $(\mathcal{M}_{\text{BC}} - c)$ is Hilbert-Schmidt. The main tool to prove that the BC are satisfied is this property. An operator that possesses the Hilbert-Schmidt property “feels the boundary” of Ω . For the sake of clarity, we restrict the discussion to the case of the Dirichlet BC.

Unlike differential operators, integral operators can increase the regularity of the function on which they act. More precisely, given $u^{\mathbb{D}}(\cdot, t) \in L^2(\Omega)$, the function $(\mathcal{M}_{\mathbb{D}} - c)u^{\mathbb{D}}(x, t)$ has an extension to a continuous function on $\overline{\Omega}$ for $t \in [0, T]$. Hence, the boundary value can be obtained by simply taking the limit as shown in (3.2). Furthermore, for the Neumann BC, the function $(\mathcal{M}_{\mathbb{N}} - c)u^{\mathbb{N}}(x, t)$ has an extension to a continuously differentiable function on $\overline{\Omega}$ for $t \in [0, T]$. Hence, the boundary value can be obtained by simply taking the limit of the derivative as shown in (3.3). In conclusion, the Hilbert-Schmidt property is the mechanism that guarantees the required regularity to enforce the BC.

The operator $\mathcal{M}_{\mathbb{D}}$ acts on $u^{\mathbb{D}}(\cdot, t) \in L^2(\Omega)$, but the space $L^2(\Omega)$ altogether ignores the values of $u^{\mathbb{D}}(\cdot, t)$ on the boundary of Ω . Next, take a closer look at the boundary behavior of the governing equation (1.1a). To ensure that the limits of the left hand side of (1.1a) exist, write them as

$$\lim_{x \rightarrow \pm 1} u_{tt}^{\mathbb{D}}(x, t) + \lim_{x \rightarrow \pm 1} (\mathcal{M}_{\mathbb{D}} - c)u^{\mathbb{D}}(x, t) + c \lim_{x \rightarrow \pm 1} u^{\mathbb{D}}(x, t) = \lim_{x \rightarrow \pm 1} b^{\mathbb{D}}(x, t).$$

Since (1.1) is a second order initial value problem in time, it naturally assumes the existence of $\lim_{x \rightarrow \pm 1} u_{tt}^{\mathbb{D}}(x, t)$, $t \in [0, T]$ and $\lim_{x \rightarrow \pm 1} u^{\mathbb{D}}(x, t)$ is provided as boundary data for all $t \in [0, T]$. One crucial question remains: Why do the limits

$$\lim_{x \rightarrow \pm 1} (\mathcal{M}_{\mathbb{D}} - c)u^{\mathbb{D}}(x, t) \tag{4.1}$$

exist? The answer is due to a subtle point in our construction. As we mentioned above, the bounded operator $\mathcal{M}_{\mathbb{D}}$ after subtracting c , i.e., $\mathcal{M}_{\mathbb{D}} - c$, possesses the Hilbert-Schmidt property. Consequently, due to the aforementioned continuous extension, the limits in (4.1) exist and in fact are equal to 0. To see the latter, we expand $u^{\mathbb{D}}$ in the Hilbert basis as

$$u^{\mathbb{D}}(x, t) = \sum_{k=1}^{\infty} \langle e_k^{\mathbb{D}} | u^{\mathbb{D}} \rangle e_k^{\mathbb{D}}(x).$$

By the spectral theorem for bounded operators, we can reproduce the same limit result in (3.2)

$$\begin{aligned}
\lim_{x \rightarrow \pm 1} (\mathcal{M}_D - c) u^D(x, t) &= \lim_{x \rightarrow \pm 1} \sum_{k=1}^{\infty} (\lambda_k(\mathcal{M}_D) - c) \langle e_k^D | u^D \rangle e_k^D(x) \\
&= \sum_{k=1}^{\infty} (\lambda_k(\mathcal{M}_D) - c) \langle e_k^D | u^D \rangle \underbrace{\lim_{x \rightarrow \pm 1} e_k^D(x)}_{= 0} \\
&= 0
\end{aligned} \tag{4.2}$$

The interchange of $\lim_{x \rightarrow \pm 1}$ with $\sum_{k=1}^{\infty}$ is justified by the uniform convergence due to the Hilbert-Schmidt property. For details, see [2].

Two important consequences follow. First, since $\lim_{x \rightarrow \pm 1} u^D(x, t)$ is assumed to exist for all $t \in [0, T]$, (4.1) implies that

$$\lim_{x \rightarrow \pm 1} \mathcal{M}_D u^D(x, t) = c \lim_{x \rightarrow \pm 1} u^D(x, t). \tag{4.3}$$

Second, a compatibility condition arises. Since we proved that the limits of the left hand side of (1.1a) exist, the governing equation (1.1a) becomes well-defined if we admit only a forcing function $b^D(\cdot, t) \in L^2(\Omega)$ that satisfies the compatibility condition:

$$\lim_{x \rightarrow \pm 1} b^D(x, t) = \lim_{x \rightarrow \pm 1} u_{tt}^D(x, t) + c \lim_{x \rightarrow \pm 1} u^D(x, t), \quad t \in [0, T].$$

For the compatibility condition of the stationary problem, see [4, Sec. 5].

4.1. Uniform Convergence and the Classical Solutions. Our nonlocal problem requires continuity at corner points $(\pm 1, 0)$ as pointed out in Remark 3.1. Thanks to uniform convergence guaranteed by the Hilbert-Schmidt property, the BC are automatically satisfied. The situation is different in the classical problem. There is no continuity requirement at corner points. This provides the freedom that initial conditions can disagree with the BC. However, the classical problem suffers from a major complication. The solutions do not guarantee that the BC are satisfied unless a uniform convergence of the series solution is in place. Even for initial value problems, uniform convergence of a series representation is a requirement for obtaining a solution to the classical wave equation [11, p. 29]. Typically, a series solution must satisfy the Weirstrass M -test to guarantee uniform convergence; see [15, Sec. 18.3.2]. Since this is not always the case, the series solutions qualify only as formal solutions [15, p. 980].

4.2. The Hilbert-Schmidt Property, Solution Operators, and Boundary Conditions. The explicit expression of the solution to (1.1) is given as

$$u^D(x, t) = \cos(t\sqrt{\mathcal{M}_D})\phi_D(x) + \frac{\sin(t\sqrt{\mathcal{M}_D})}{\sqrt{\mathcal{M}_D}}\psi_D(x) + \int_0^t \frac{\sin((t-\tau)\sqrt{\mathcal{M}_D})}{\sqrt{\mathcal{M}_D}} b^D(x, \tau) d\tau. \tag{4.4}$$

See [2, Eq.(16) and Thm. 8] and [10, Thm. 1 and Thm. 3] for the expressions for bounded and unbounded domain, respectively. Giving a rigorous proof for the fact that BC are satisfied for all $t \in [0, T]$ calls for establishing the Hilbert-Schmidt property of the solution operators. The solution

representation in (4.4) suggests defining the following solution operators.

$$\begin{aligned} g_{\mathbb{D},0}(\mathcal{M}_{\mathbb{D}})\phi_{\mathbb{D}}(x) &:= \cos(t\sqrt{\mathcal{M}_{\mathbb{D}}})\phi_{\mathbb{D}}(x) \\ g_{\mathbb{D},1}(\mathcal{M}_{\mathbb{D}})\psi_{\mathbb{D}}(x) &:= \frac{\sin(t\sqrt{\mathcal{M}_{\mathbb{D}}})}{\sqrt{\mathcal{M}_{\mathbb{D}}}}\psi_{\mathbb{D}}(x) \\ g_{\mathbb{D},2}(\mathcal{M}_{\mathbb{D}})b^{\mathbb{D}}(x,t) &:= \int_0^t \frac{\sin((t-\tau)\sqrt{\mathcal{M}_{\mathbb{D}}})}{\sqrt{\mathcal{M}_{\mathbb{D}}}}b^{\mathbb{D}}(x,\tau) d\tau. \end{aligned}$$

Note that all solution operators are bounded functions of $\mathcal{M}_{\mathbb{D}}$; see [2, Sec. 2.5]. We decompose the solution operators in the following way to extract a Hilbert-Schmidt term:

$$g_{\mathbb{D},i}(\mathcal{M}_{\mathbb{D}}) = [g_{\mathbb{D},i}(\mathcal{M}_{\mathbb{D}}) - g_{\mathbb{D},i}(c)] + g_{\mathbb{D},i}(c), \quad i = 0, 1, 2. \quad (4.5)$$

In [2, Sec. 3.1], we proved that the term $[g_{\mathbb{D},i}(\mathcal{M}_{\mathbb{D}}) - g_{\mathbb{D},i}(c)]$ is a Hilbert-Schmidt operator. Hence, $[g_{\mathbb{D},i}(\mathcal{M}_{\mathbb{D}}) - g_{\mathbb{D},i}(c)]v(x)$ has an extension to a continuous function on $\bar{\Omega}$. As a result, the following limits all exist and are equal to zero

$$\lim_{x \rightarrow \pm 1} [g_{\mathbb{D},0}(\mathcal{M}_{\mathbb{D}}) - g_{\mathbb{D},0}(c)]\phi_{\mathbb{D}}(x) = 0 \quad (4.6)$$

$$\lim_{x \rightarrow \pm 1} [g_{\mathbb{D},1}(\mathcal{M}_{\mathbb{D}}) - g_{\mathbb{D},1}(c)]\psi_{\mathbb{D}}(x) = 0 \quad (4.7)$$

$$\lim_{x \rightarrow \pm 1} [g_{\mathbb{D},2}(\mathcal{M}_{\mathbb{D}}) - g_{\mathbb{D},2}(c)]b^{\mathbb{D}}(x,t) = 0. \quad (4.8)$$

To prove the latter for (4.6), we proceed similarly as for the result in (4.2). We apply the spectral theorem for bounded operators and obtain

$$\begin{aligned} \lim_{x \rightarrow \pm 1} [g_{\mathbb{D},0}(\mathcal{M}_{\mathbb{D}}) - g_{\mathbb{D},0}(c)]\phi_{\mathbb{D}}(x) &= \lim_{x \rightarrow \pm 1} \sum_{k=1}^{\infty} (g_{\mathbb{D},0}(\lambda_k(\mathcal{M}_{\mathbb{D}})) - g_{\mathbb{D},0}(c)) \langle e_k^{\mathbb{D}} | u^{\mathbb{D}} \rangle e_k^{\mathbb{D}}(x) \\ &= \sum_{k=1}^{\infty} (g_{\mathbb{D},0}(\lambda_k(\mathcal{M}_{\mathbb{D}})) - g_{\mathbb{D},0}(c)) \langle e_k^{\mathbb{D}} | u^{\mathbb{D}} \rangle \underbrace{\lim_{x \rightarrow \pm 1} e_k^{\mathbb{D}}(x)}_{=0} \\ &= 0. \end{aligned}$$

Again, the interchange of $\lim_{x \rightarrow \pm 1}$ with $\sum_{k=1}^{\infty}$ is justified by the uniform convergence due to the Hilbert-Schmidt property of the operator $[g_{\mathbb{D},0}(\mathcal{M}_{\mathbb{D}}) - g_{\mathbb{D},0}(c)]$. Consequently, similar to (4.3), we arrive at

$$\lim_{x \rightarrow \pm 1} g_{\mathbb{D},0}(\mathcal{M}_{\mathbb{D}})\phi_{\mathbb{D}}(x) = g_{\mathbb{D},0}(c) \lim_{x \rightarrow \pm 1} \phi_{\mathbb{D}}(x) = \cos(t\sqrt{c})\phi_{\mathbb{D}}(\pm 1).$$

When we write the solution expression in (4.4) in terms of the solution operators and, for each term, utilize the decomposition (4.5), we arrive at

$$\begin{aligned} u^{\mathbb{D}}(x,t) &= \cos(t\sqrt{c})\phi_{\mathbb{D}}(x) + \frac{\sin(t\sqrt{c})}{\sqrt{c}}\psi_{\mathbb{D}}(x) + \int_0^t \frac{\sin((t-\tau)\sqrt{c})}{\sqrt{c}}b^{\mathbb{D}}(x,\tau) d\tau + \\ &[g_{\mathbb{D},0}(\mathcal{M}_{\mathbb{D}}) - g_{\mathbb{D},0}(c)]\phi_{\mathbb{D}}(x) + [g_{\mathbb{D},1}(\mathcal{M}_{\mathbb{D}}) - g_{\mathbb{D},1}(c)]\psi_{\mathbb{D}}(x) + [g_{\mathbb{D},2}(\mathcal{M}_{\mathbb{D}}) - g_{\mathbb{D},2}(c)]b^{\mathbb{D}}(x,t). \end{aligned}$$

Taking $\lim_{x \rightarrow \pm 1}$, using (4.6), (4.7), (4.8), and making all the necessary choices in (3.10), the expression of the solution on the boundary takes the form

$$u_{\pm}^{\mathbb{D}}(t) = \cos(t\sqrt{c})\alpha_{\pm}^{\mathbb{D}}(0) + \frac{\sin(t\sqrt{c})}{\sqrt{c}} \frac{d\alpha_{\pm}^{\mathbb{D}}}{dt}(0) + \int_0^t \frac{\sin((t-\tau)\sqrt{c})}{\sqrt{c}} \left(\frac{d^2\alpha_{\pm}^{\mathbb{D}}}{dt^2}(\tau) + c\alpha_{\pm}^{\mathbb{D}}(\tau) \right) d\tau. \quad (4.9)$$

Applying integration by parts twice on (4.9) eventually leads to satisfying the BC:

$$u_{\pm}^{\text{D}}(t) = \alpha_{\pm}^{\text{D}}(t), \quad t \in [0, T].$$

5. EXACT SOLUTIONS WITH HOMOGENEOUS BC

Thanks to functional calculus, it is possible to find exact solutions to (1.1) and (1.2). We can generalize the solution operators in (4.4) and the expressions for the solution to (1.1) and (1.2) are given as [2, 10]

$$u^{\text{BC}}(x, t) = \cos(t\sqrt{\mathcal{M}_{\text{BC}}})\phi_{\text{BC}}(x) + \frac{\sin(t\sqrt{\mathcal{M}_{\text{BC}}})}{\sqrt{\mathcal{M}_{\text{BC}}}}\psi_{\text{BC}}(x) + \int_0^t \frac{\sin((t-\tau)\sqrt{\mathcal{M}_{\text{BC}}})}{\sqrt{\mathcal{M}_{\text{BC}}}}b^{\text{BC}}(x, \tau) d\tau. \quad (5.1)$$

Using the Hilbert basis and the spectral theorem for bounded operators, expression (5.1) can be written in terms of the following series representation.

$$u^{\text{BC}}(x, t) = \sum_{k \in \mathbb{N}_{\text{BC}}} \cos(t\sqrt{f_{\text{BC}}(\lambda_k^{\text{BC}})}) \langle e_k^{\text{BC}} | \phi_{\text{BC}} \rangle e_k^{\text{BC}}(x) + \sum_{k \in \mathbb{N}_{\text{BC}}} \frac{\sin(t\sqrt{f_{\text{BC}}(\lambda_k^{\text{BC}})})}{\sqrt{f_{\text{BC}}(\lambda_k^{\text{BC}})}} \langle e_k^{\text{BC}} | \psi_{\text{BC}} \rangle e_k^{\text{BC}}(x) + \sum_{k \in \mathbb{N}_{\text{BC}}} \left[\int_0^t \frac{\sin((t-\tau)\sqrt{f_{\text{BC}}(\lambda_k^{\text{BC}})})}{\sqrt{f_{\text{BC}}(\lambda_k^{\text{BC}})}} \langle e_k^{\text{BC}} | b^{\text{BC}}(\tau) \rangle d\tau \right] e_k^{\text{BC}}(x).$$

The series can be collapsed by using the orthonormality of e_k^{BC} . For instance, the choice of

$$b^{\text{BC}}(x, t) \equiv 0, \quad \phi_{\text{BC}}(x) = e_m^{\text{BC}}(x), \quad \psi_{\text{BC}}(x) \equiv 0, \quad (5.2)$$

for some $m \in \mathbb{N} \setminus \{0\}$, leads to

$$u^{\text{BC}}(x, t) = \cos(t\sqrt{f_{\text{BC}}(\lambda_m^{\text{BC}})})e_m^{\text{BC}}(x).$$

5.1. Classical Exact Solutions with Homogeneous BC. We also study the local analogs of the problems (1.1) and (1.2). We consider the classical wave equation with homogeneous Dirichlet and Neumann BC with the same choice given in (5.2)

$$\begin{aligned} u_{tt}^{\text{BC}}(x, t) - \frac{4}{\pi^2}u_{xx}^{\text{BC}}(x, t) &= 0, \quad (x, t) \in \Omega \times (0, T), \\ u^{\text{D}}(\pm 1, t) &= 0 \quad \text{or} \quad u_x^{\text{N}}(\pm 1, t) = 0, \\ u^{\text{BC}}(x, 0) &= e_m^{\text{BC}}(x), \\ u_t^{\text{BC}}(x, 0) &= 0, \end{aligned} \quad (5.3)$$

for some $m \in \mathbb{N} \setminus \{0\}$. It is possible to obtain a closed form solution using d'Alembert's formula together with the method of images or reflections. After some algebra, we obtain

$$u^{\text{BC}}(x, t) = \cos(t\sqrt{m^2})e_m^{\text{BC}}(x).$$

Since the classical governing equations (5.3) contain the classical operators A_{BC} , the regulating function is nothing but the identity function. Using the expression of the spectrum $\sigma(A_{\text{BC}}) = \{k^2 : k \in \mathbb{N}_{\text{BC}}\}$, we have

$$f_{\text{BC}}^{\text{classi}}(\lambda_k^{\text{BC}}) = \lambda_k^{\text{BC}} = k^2, \quad k \in \mathbb{N}_{\text{BC}}.$$

Even though $f_{\text{BC}}^{\text{classi}} : \sigma(A_{\text{BC}}) \rightarrow \mathbb{R}$ is not a bounded function, $\cos(t\sqrt{f_{\text{BC}}^{\text{classi}}(\lambda_k^{\text{BC}})})$ is a bounded function of λ_k^{BC} . The solution expression obtained from the formula (5.1) still captures the expression obtained from d'Alembert's formula due to the spectral theorem for bounded operators.

6. EXACT SOLUTIONS WITH INHOMOGENEOUS BC

We treat inhomogeneous BC by the method of shifting the data [19, p. 149]. A shift function $G^{\text{BC}}(x, t)$ is designed to satisfy the BC and is defined as

$$G^{\text{D}}(\pm 1, t) = \alpha_{\pm}^{\text{D}}(t) \quad \text{and} \quad G_x^{\text{N}}(\pm 1, t) = \alpha_{\pm}^{\text{N}}(t) \quad (6.1)$$

$G^{\text{BC}}(x, t)$ can be any function that satisfies (6.1). A practical choice is

$$G^{\text{D}}(x, t) = \frac{1-x}{2}\alpha_{-}^{\text{D}}(t) + \frac{1+x}{2}\alpha_{+}^{\text{D}}(t), \quad (6.2)$$

$$G^{\text{N}}(x, t) = -\frac{(1-x)^2}{4}\alpha_{-}^{\text{N}}(t) + \frac{(1+x)^2}{4}\alpha_{+}^{\text{N}}(t). \quad (6.3)$$

The boundary data are assumed to have the following regularity

$$\alpha_{\pm}^{\text{D}} \in \mathcal{C}^2([0, T]) \quad \text{and} \quad \alpha_{\pm}^{\text{N}} \in \mathcal{C}^3([0, T]). \quad (6.4)$$

As a result of (6.4), the shift function should have the following regularity.

$$G^{\text{D}} \in \mathcal{C}^2([0, T], L^2(\Omega)) \quad \text{and} \quad G^{\text{N}} \in \mathcal{C}^3([0, T], L^2(\Omega)).$$

Here, for instance by $G^{\text{D}} \in \mathcal{C}^2([0, T], L^2(\Omega))$, we mainly mean a twice continuously differentiable function in the time variable and a square integrable function in the space variable. Eventually, an equivalent IVP with homogeneous BC is obtained by defining

$$w^{\text{BC}}(x, t) := u^{\text{BC}}(x, t) - G^{\text{BC}}(x, t). \quad (6.5)$$

Combining (1.1b) and (1.2b) with (6.1), we obtain the homogeneous BC, i.e., $w^{\text{D}}(\pm 1, t) = 0$ and $w_x^{\text{N}}(\pm 1, t) = 0$. Substituting the expression for $u^{\text{BC}}(x, t)$ from (6.5) into (1.1) and (1.2), we arrive at the equivalent problem with homogeneous BC:

$$\begin{aligned} w_{tt}^{\text{BC}}(x, t) + \mathcal{M}_{\text{BC}} w^{\text{BC}}(x, t) &= b^{\text{BC}, w}(x, t), \quad (x, t) \in \Omega \times (0, T), \\ w^{\text{D}}(\pm 1, t) &= 0 \quad \text{or} \quad w_x^{\text{N}}(\pm 1, t) = 0, \\ w^{\text{BC}}(x, 0) &= \phi_{\text{BC}}^w(x), \\ w_t^{\text{BC}}(x, 0) &= \psi_{\text{BC}}^w(x), \end{aligned}$$

where we define

$$\begin{aligned} b^{\text{BC}, w}(x, t) &:= b^{\text{BC}}(x, t) - G_{tt}^{\text{BC}}(x, t) - \mathcal{M}_{\text{BC}} G^{\text{BC}}(x, t) \\ \phi_{\text{BC}}^w(x) &:= \phi_{\text{BC}}(x) - G^{\text{BC}}(x, 0) \\ \psi_{\text{BC}}^w(x) &:= \psi_{\text{BC}}(x) - G_t^{\text{BC}}(x, 0). \end{aligned}$$

Then, the explicit expression for the solution $u^{\text{BC}}(x, t)$ from (5.1) takes the form

$$\begin{aligned} u^{\text{BC}}(x, t) &= G^{\text{BC}}(x, t) + \cos(t\sqrt{\mathcal{M}_{\text{BC}}})(\phi_{\text{BC}}(x) - G^{\text{BC}}(x, 0)) + \\ &\frac{\sin(t\sqrt{\mathcal{M}_{\text{BC}}})}{\sqrt{\mathcal{M}_{\text{BC}}}}(\psi_{\text{BC}}(x) - G_t^{\text{BC}}(x, 0)) + \\ &\int_0^t \frac{\sin((t-\tau)\sqrt{\mathcal{M}_{\text{BC}}})}{\sqrt{\mathcal{M}_{\text{BC}}}}(b^{\text{BC}}(x, \tau) - G_{tt}^{\text{BC}}(x, \tau) - \mathcal{M}_{\text{BC}}G^{\text{BC}}(x, \tau)) d\tau. \end{aligned}$$

The corresponding series representation takes the form

$$\begin{aligned} u^{\text{BC}}(x, t) &= G^{\text{BC}}(x, t) + \sum_{k \in \mathbb{N}_{\text{BC}}} \cos(t\sqrt{f_{\text{BC}}(\lambda_k^{\text{BC}})}) \langle e_k^{\text{BC}} | \phi_{\text{BC}} - G^{\text{BC}}(\cdot, 0) \rangle e_k^{\text{BC}}(x) + \\ &\sum_{k \in \mathbb{N}_{\text{BC}}} \frac{\sin(t\sqrt{f_{\text{BC}}(\lambda_k^{\text{BC}})})}{\sqrt{f_{\text{BC}}(\lambda_k^{\text{BC}})}} \langle e_k^{\text{BC}} | \psi_{\text{BC}} - G_t^{\text{BC}}(\cdot, 0) \rangle e_k^{\text{BC}}(x) + \\ &\sum_{k \in \mathbb{N}_{\text{BC}}} \left[\int_0^t \frac{\sin((t-\tau)\sqrt{f_{\text{BC}}(\lambda_k^{\text{BC}})})}{\sqrt{f_{\text{BC}}(\lambda_k^{\text{BC}})}} \langle e_k^{\text{BC}} | b^{\text{BC}}(\cdot, \tau) - G_{tt}^{\text{BC}}(\cdot, \tau) - \mathcal{M}_{\text{BC}}G^{\text{BC}}(\cdot, \tau) \rangle d\tau \right] e_k^{\text{BC}}(x). \end{aligned} \quad (6.6)$$

To find an exact solution with inhomogeneous BC, we make the following choices for the series representation (6.6):

$$\begin{aligned} b^{\text{BC}}(x, t) &= G_{tt}^{\text{BC}}(x, t) + \mathcal{M}_{\text{BC}}G^{\text{BC}}(x, t), \\ \phi_{\text{BC}}(x) &= G^{\text{BC}}(x, 0), \\ \psi_{\text{BC}}(x) &= G_t^{\text{BC}}(x, 0). \end{aligned} \quad (6.7)$$

With this choice, note that all the terms in (6.6) vanish except the first term. Eventually, we arrive at the exact solution

$$u^{\text{BC}}(x, t) = G^{\text{BC}}(x, t). \quad (6.8)$$

One can easily construct other exact solutions by making different choices in (6.7).

7. THE CHOICE OF KERNEL FUNCTIONS, SCALING, AND THE DISCRETIZATION

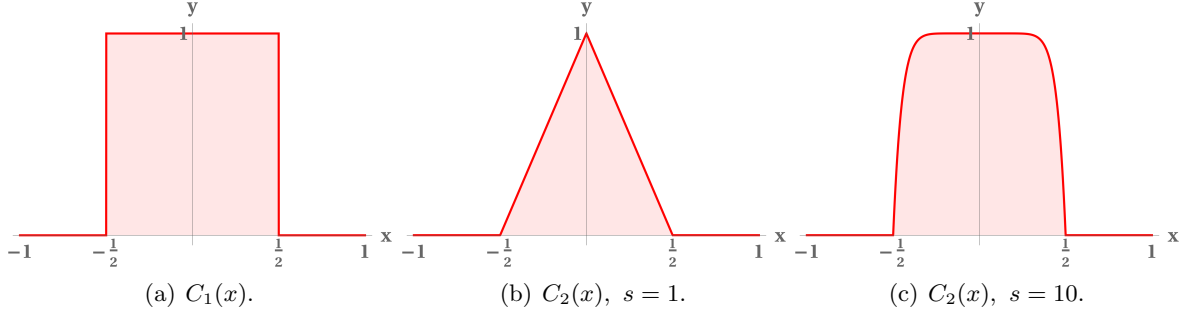
A collocation method with piecewise linear nodal basis functions is employed to discretize the governing equations (1.1a) and (1.2a). A family of kernel functions with horizon δ is chosen as

$$\begin{aligned} C_1(x) &:= \begin{cases} 1, & x \in (-\delta, \delta) \\ 0, & \text{otherwise,} \end{cases} \\ C_2(x) &:= \begin{cases} 1 - \left|\frac{x}{\delta}\right|^s, & x \in (-\delta, \delta) \\ 0, & \text{otherwise,} \end{cases} \end{aligned}$$

with $s > 0$. Next, we want to elaborate on the choice of kernel functions. For univariate and bivariate kernel functions, see Fig. 7.1 and Fig. 7.2, respectively. First note that

$$\lim_{s \rightarrow \infty} C_2(x) = C_1(x), \quad (7.1)$$

such that C_2 is a family that approaches C_1 . The parameter s associated with the C_2 family provides a way to monitor matrix properties as $s \rightarrow \infty$.

FIGURE 7.1. Plot of the univariate kernel function $C(x)$ with $\delta = 2^{-1}$.

After suitable scaling, in \mathbb{R} , it is well-known that the peridynamic governing operator converges to the Laplace operator as $\delta \rightarrow 0$ [9]. When collocation with piecewise linear nodal basis is used, the suitable scaling turns out to be

$$\text{scaling} = \frac{2}{\delta^3}. \quad (7.2)$$

The scaling (7.2) is always inserted in the governing operators to capture the local operator. Likewise, the discretized nonlocal operator should capture the discretized Laplace operator in some sense. With the choice of C_1 as a kernel function, when $\delta = h$, except first and last rows, the discretized operator satisfies

$$\frac{2}{\delta^3} \mathcal{M}_{\text{BC}}^h = \frac{1}{h^2} \text{tridiag}(-1, 2, -1).$$

Similarly when $\delta = h$, the kernel function C_2 leads to

$$\frac{2}{\delta^3} \mathcal{M}_{\text{BC}}^h = \frac{1}{h^2} \text{tridiag}\left(-\frac{s}{s+2}, \frac{2s}{s+2}, -\frac{s}{s+2}\right).$$

Similar to convergence in (7.1), the discretization of \mathcal{M}_{BC} with C_2 converges to that with C_1 . More precisely,

$$\lim_{s \rightarrow \infty} \text{tridiag}\left(-\frac{s}{s+2}, \frac{2s}{s+2}, -\frac{s}{s+2}\right) = \text{tridiag}(-1, 2, -1).$$

Hence, capturing the discretized Laplace operator in some sense corresponds to obtaining $\frac{1}{h^2} \text{tridiag}(-1, 2, -1)$ or attaining it as $s \rightarrow \infty$ in our context.

7.1. The Zero Row Sum Property. Note that the constant function $u(x, t) \equiv k$ is in the kernel of the \mathcal{M}_{N} operator. Since $\mathcal{M}_{\text{N}} k \equiv 0$, the discretized operator \mathcal{M}_{N}^h satisfies

$$\mathcal{M}_{\text{N}}^h \mathbf{1}_h = \mathbf{0}_h.$$

In other words, \mathcal{M}_{N}^h has zero row sum property for all of its rows. Since \mathcal{M}_{N} and \mathcal{M}_{D} agree in the bulk, the zero row sum property holds for \mathcal{M}_{D}^h for all rows corresponding to the bulk. We pay a special attention to maintain the zero row sum property at machine precision. One crucial step is to incorporate the scaling (7.2) after $\mathcal{M}_{\text{BC}}^h u_h$ takes place. See how we reflect this to our time stepping iteration:

$$\begin{aligned} v^n &= \mathcal{M}_{\text{BC}}^h u_h^n, \\ u_h^{n+1} &= 2u_h^n - u_h^{n-1} + \frac{1}{2} dt^2 \left(b_h^n - \frac{2}{\delta^3} v^n \right), \quad n = 1, \dots \end{aligned}$$

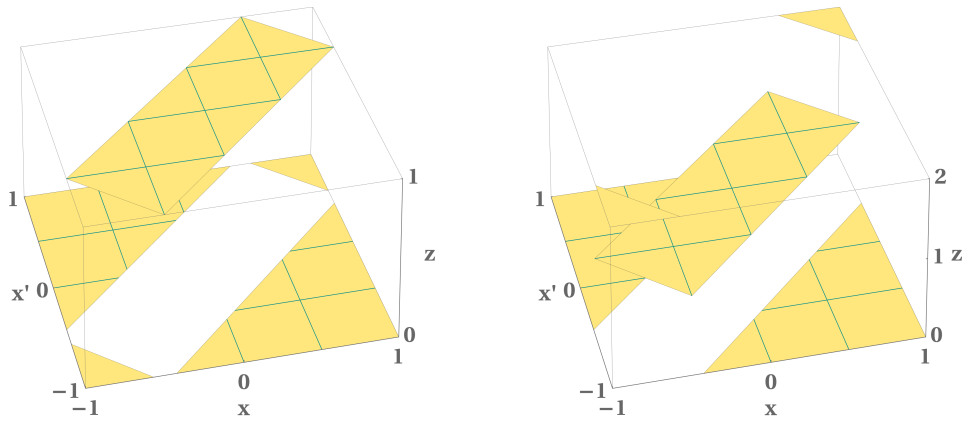
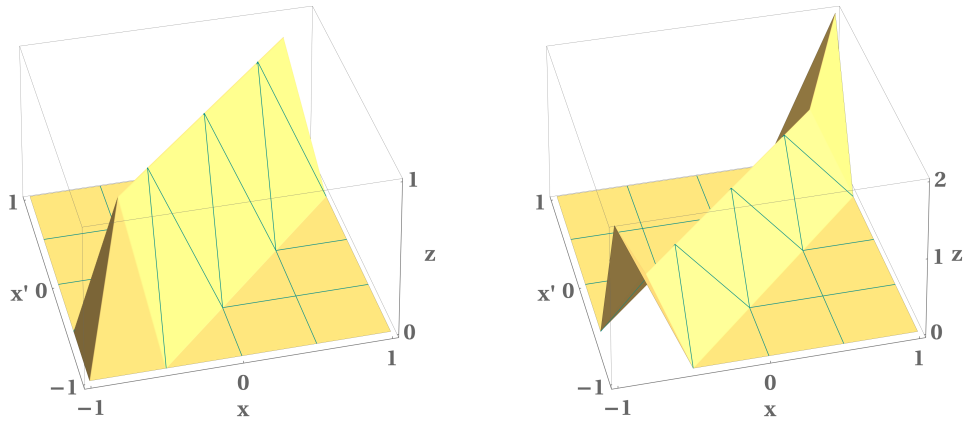
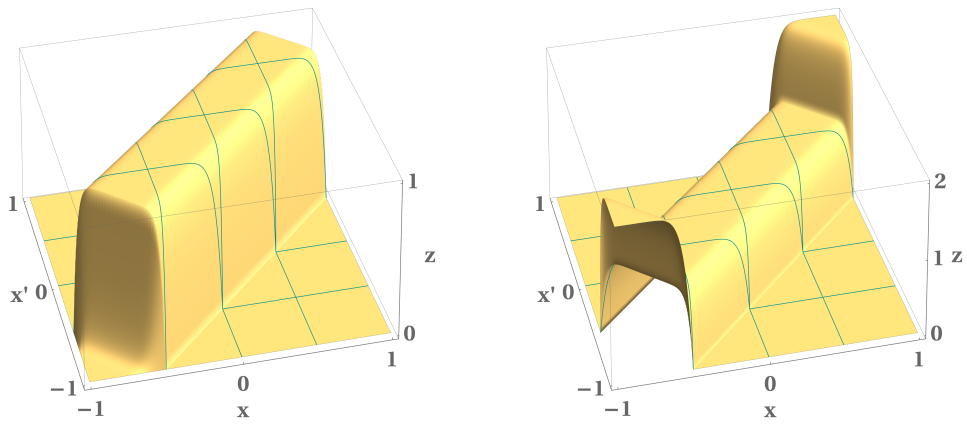
(a) $C(x) = C_1(x)$.(b) $C(x) = C_2(x)$, $s = 1$.(c) $C(x) = C_2(x)$, $s = 10$.

FIGURE 7.2. Plot of the bivariate kernel functions $K_D(x, x')$ (left) and $K_N(x, x')$ (right) with $\delta = 2^{-1}$.

Otherwise, for small δ , round-off errors spoil the zero row sum property which leads to distortions in the wave pattern.

8. INTERPOLATION STRATEGY TO ENFORCE NEUMANN BOUNDARY CONDITION

The expression (3.9), which determines the suitable forcing function to enforce Neumann BC, involves $b_x^N(\pm 1, t)$. On the other hand, the forcing function in the governing equation (1.2a) involves $b^N(\pm 1, t)$. We will prescribe an interpolation strategy to find the appropriate value of $b^N(\pm 1, t)$ that uses the value of $b_x^N(\pm 1, t)$. For sake of simplicity, let us consider only the BC on the left boundary point, i.e., of $x = x_1 = -1$, and the kernel function $C_1(x)$.

Using nodal collocation with Lagrange basis functions, the discrete solution takes the form

$$u_h^N(x, t) = \sum_{j=1}^N u_h^N(x_j, t) \phi_j(x).$$

After discretization and incorporating the scaling (7.2), the governing equation (1.2a) becomes

$$\frac{2}{\delta^3} c_1 \sum_{j=1}^N u_h^N(x_j, t) \phi_j(x) - \sum_{j=1}^N u_h^N(x_j, t) \int_{\Omega} \frac{2}{\delta^3} K_N(x' - x) \phi_j(x') dx' = b^N(x, t). \quad (8.1)$$

On substituting $x = x_1$, incorporating $c_1 := \int_{\Omega} C_1(x) dx = 2\delta$, and collapsing the sum only in the first term, the expression (8.1) reduces to

$$\frac{4}{\delta^2} u_h^N(x_1, t) - \sum_{j=1}^N u_h^N(x_j, t) \int_{\Omega} \frac{2}{\delta^3} K_N(x' - x_1) \phi_j(x') dx' = b^N(x_1, t). \quad (8.2)$$

The kernel function $K_N(x' - x_1)$ has the support of $[x_1, x_1 + \delta]$ and becomes identically the constant function 2. Hence,

$$K_N(x' - x_1) = 2 \chi_{[x_1, x_1 + \delta]}.$$

Note that only the supports of ϕ_1 and ϕ_2 intersect $[x_1, x_1 + \delta]$. The equation (8.2) reduces to

$$\frac{4}{\delta^2} u_h^N(x_1, t) - \frac{2}{\delta^3} u_h^N(x_1, t) \int_{[x_1, x_1 + \delta]} 2 \phi_1(x') dx' - \frac{2}{\delta^3} u_h^N(x_1 + \delta, t) \int_{[x_1, x_1 + \delta]} 2 \phi_2(x') dx' = b^N(x_1, t).$$

After using

$$\int_{[x_1, x_1 + \delta]} \phi_1(x') dx' = \int_{[x_1, x_1 + \delta]} \phi_2(x') dx' = \frac{\delta}{2},$$

we obtain

$$\frac{2}{\delta^2} u_h^N(x_1, t) - \frac{2}{\delta^2} u_h^N(x_1 + \delta, t) = b^N(x_1, t). \quad (8.3)$$

We arrive at the critical interpolation step: What should the choice of $b^N(x_1, t)$ be? Let us see why the choice of

$$b^N(x_1, t) := -\frac{\delta}{2} b_x^N(x_1, t) = -\frac{\delta}{2} \left(\frac{d^2 \alpha_-^N}{dt^2}(t) + \frac{2}{\delta^3} c_1 \alpha_-^N(t) \right) \quad (8.4)$$

is suitable. After some algebra and with the choice in (8.4), the expression in (8.3) is equivalent to

$$\frac{u_h^N(x_1 + \delta, t) - u_h^N(x_1, t)}{\delta} = \frac{\delta^2}{4} \frac{d^2 \alpha_-^N}{dt^2}(t) + \alpha_-^N(t),$$

which leads to

$$\frac{\partial u_h^N}{\partial x}(x_1, t) = \lim_{\delta \rightarrow 0} \frac{u_h^N(x_1 + \delta, t) - u_h^N(x_1, t)}{\delta} = \alpha_-^N(t).$$

Consequently, the choice (8.4) guarantees that the BC is satisfied with $\mathcal{O}(\delta^2)$ accuracy as $\delta \rightarrow 0$.

When the kernel function C_1 is used, we reported the choice of b^N in (8.4). When C_2 is used, the choice becomes

$$b^N(x_1, t) := -\frac{\delta}{2} \left(\frac{s+1}{s+2} \right) b_x^N(x_1, t) = -\frac{\delta}{2} \left(\frac{s+1}{s+2} \right) \left(\frac{d^2 \alpha_-^N}{dt^2}(t) + \frac{2}{\delta^3} c_2 \alpha_-^N(t) \right),$$

where $c_2 := \int_{\Omega} C_2(x) dx = 2\delta s/(s+1)$.

9. IMPLEMENTATION AND NUMERICAL EXPERIMENTS

When a uniform grid is used, the structure of the kernel function does not permit the boundary data to enter correctly, i.e., without distortion, into the bulk. Hence, we are forced to use a *fitted grid* with spacing h and δ inside and outside the bulk, respectively. Hence, grid nodes are

$$\Omega_h := \{-1, -1 + \delta, -1 + \delta + h, \dots, -h, 0, h, \dots, 1 - \delta - h, 1 - \delta, 1\}.$$

When the boundary data are homogeneous, one can use a uniform grid instead of a fitted one. Let us dwell on why fitted grid is essential for our numerical method. The boundary data reside in the first and last degrees of freedom (DOF). Hence, the first and last columns of the stiffness matrix are the most important columns for propagating data into the domain. For instance, consider the Dirichlet problem with the kernel C_1 . With a uniform grid, observe that the first/last column entries corresponding to DOF between the boundary and the bulk vanish simply due to the structure of the kernel function; see Fig. 7.2. As a result, boundary data cannot propagate into the domain. When we choose C_2 as the kernel function, those entries in the first/last column become nonzero. But, this is a partial fix because now the rows corresponding to DOF do not satisfy the zero row sum property, which gives rise to wave distortion. Consequently, the fitted grid is a requirement of the inhomogeneous boundary data.

In order to maintain regularity assumptions, the boundary data choices satisfy $\alpha_{\pm}^{\text{BC}}(t) \in \mathcal{C}^3([0, 10])$. For time integration, we employ the Newmark scheme with $\Delta t = 0.95 \times 10^{-3}$ and $\Delta t = 0.50 \times 10^{-3}$ for known and unknown solutions, respectively.

9.1. Dirichlet and Neumann Problem with Known Exact Solution. The pointwise relative error between the exact and the approximate displacement is defined as

$$e^{\text{BC}}(x_i, t_j) := \frac{G^{\text{BC}}(x_i, t_j) - u^{\text{BC}}(x_i, t_j)}{\|G^{\text{BC}}(\cdot, t_j)\|_{L^2(\Omega)}}, \quad (9.1)$$

where u^{BC} denotes the approximate displacement. On the other hand, for the Neumann problem, the relative strain error is defined as

$$e_{\text{strain}}(x_i, t_j) := \frac{G_x^N(x_i, t_j) - s(x_i, t_j)}{\|G_x^N(\cdot, t_j)\|_{L^2(\Omega)}}, \quad (9.2)$$

where $s(x_i, t_j)$ denotes the approximate strain computed by a central difference scheme.

We resort to the method of shifting the data presented in Sec. 6. The accuracy of the numerical solution is verified by setting up a test case in which the exact solution is identically equal to the

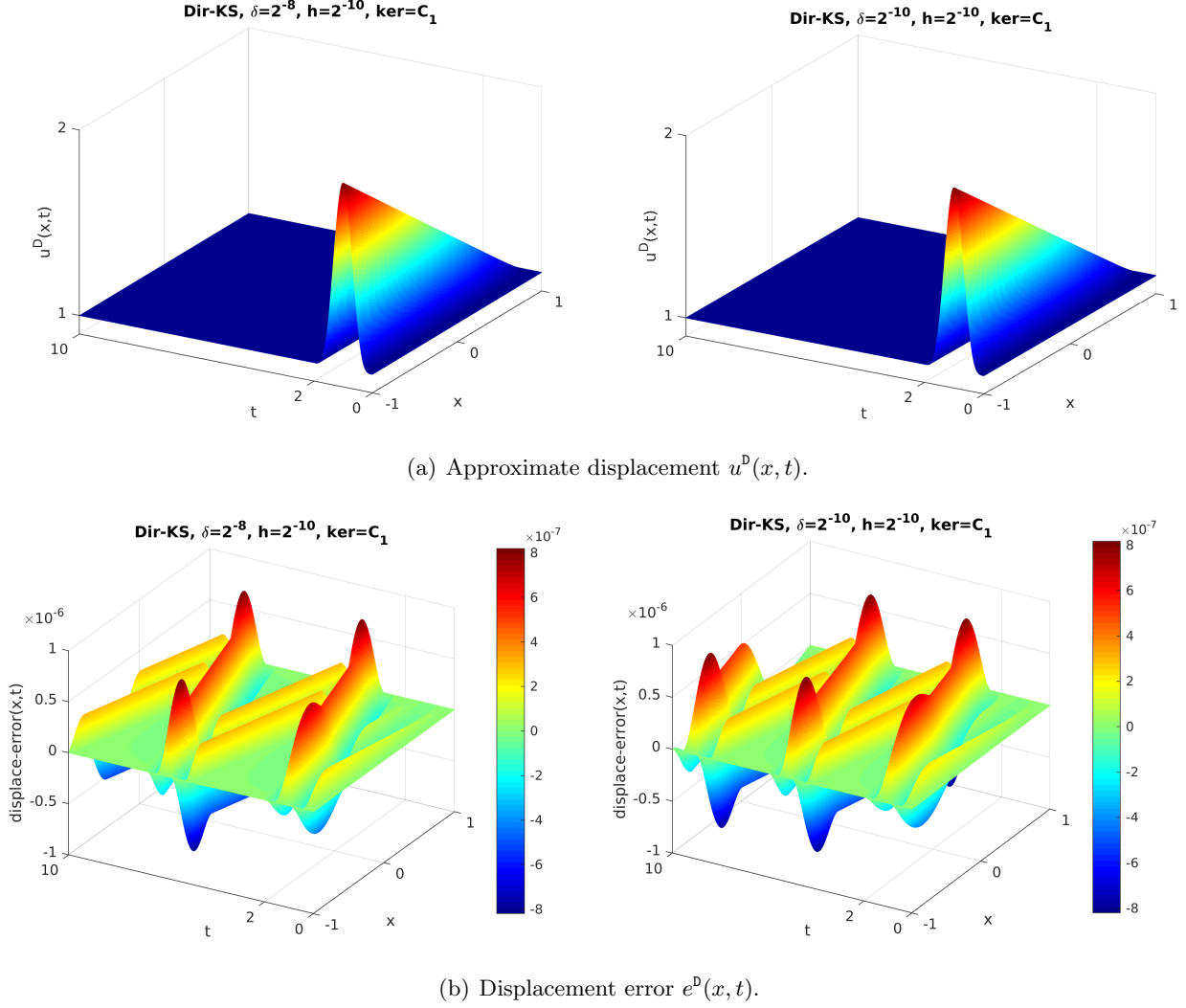


FIGURE 9.1. Displacement of the Dirichlet problem with known exact solution with $h = 2^{-10}$, $\Delta t = 0.95 \times 10^{-3}$, kernel function $C_1(x)$, and $\delta = 2^{-8}$ (left) and $\delta = 2^{-10}$ (right).

shift function as indicated in (6.8). The shift functions are chosen as the practical ones given in (6.2) and (6.3). We use the same boundary data for Dirichlet and Neumann problems:

$$\alpha_{-}^{\text{BC}}(t) := \begin{cases} \frac{1}{4}(1 - \cos(\pi t))^2 + 1, & t \in [0, 2] \\ 0, & t \in (2, 10] \end{cases} \quad \text{and} \quad \alpha_{+}^{\text{BC}}(t) := 1, \quad t \in [0, 10], \quad (9.3)$$

where

$$u^D(\pm 1, t) = \alpha_{\pm}^D(t) \quad \text{and} \quad \frac{\partial u^N}{\partial x}(\pm 1, t) = \alpha_{\pm}^N(t).$$

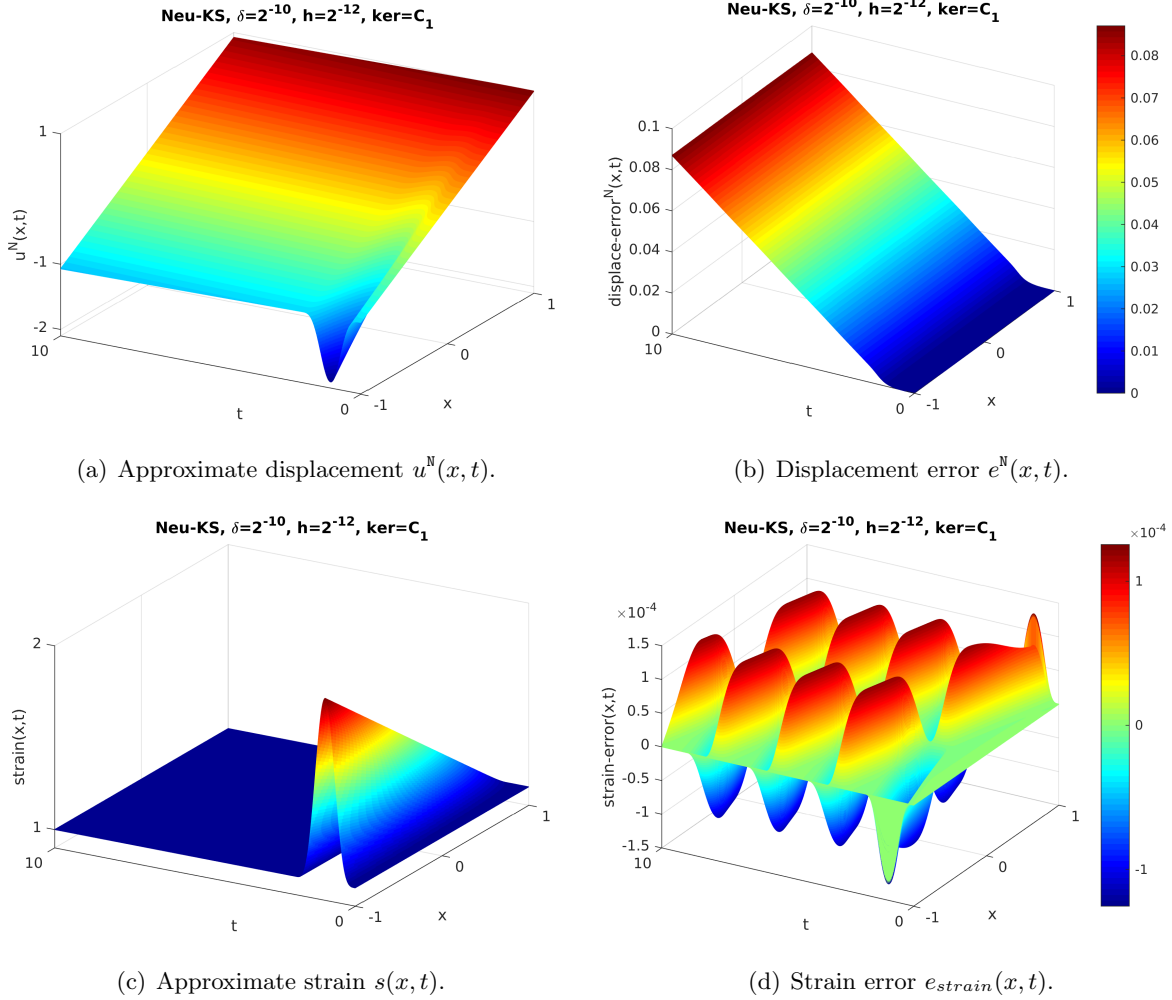


FIGURE 9.2. Displacement of the Neumann problem with known exact solution with $\delta = 2^{-10}$, $h = 2^{-12}$, $\Delta t = 0.50 \times 10^{-3}$, and kernel function $C_1(x)$.

Note that the boundary data in (9.3) is only different from that for unknown solutions in (9.4) by a shift of 1. The shift guarantees nonvanishing $\|G^{BC}(\cdot, t_j)\|_{L^2(\Omega)}$ and $\|G_x^N(\cdot, t_j)\|_{L^2(\Omega)}$ values to be able to report relative errors.

The forcing functions are chosen as

$$b^{BC}(x, t) = G_{tt}^{BC}(x, t) + \mathcal{M}_{BC} G^{BC}(x, t), \quad x \in \bar{\Omega}, \quad t \in [0, 10],$$

with a time step of $\Delta t = h = \mathcal{O}(10^{-3})$ and a grid spacing of $h = 2^{-10}$. It can be seen that the computational solutions well approximate the exact solutions; see Fig. 9.1. For the Dirichlet problem, the relative error in displacement is computed using (9.1) and is $e^D(x_i, t_j) = \mathcal{O}(10^{-6}) = \mathcal{O}(\Delta t^2 + h^2)$.

For the Neumann problem, the relative errors in displacement and strain are computed using (9.1) and (9.2), respectively. With $h = 2^{-12}$, the error observed is $e^N(x_i, t_j) = \mathcal{O}(10^{-2})$ and $e_{strain}^N(x_i, t_j) = \mathcal{O}(10^{-3})$. Due to the large displacement error, a smaller grid spacing of $h = 2^{-14}$

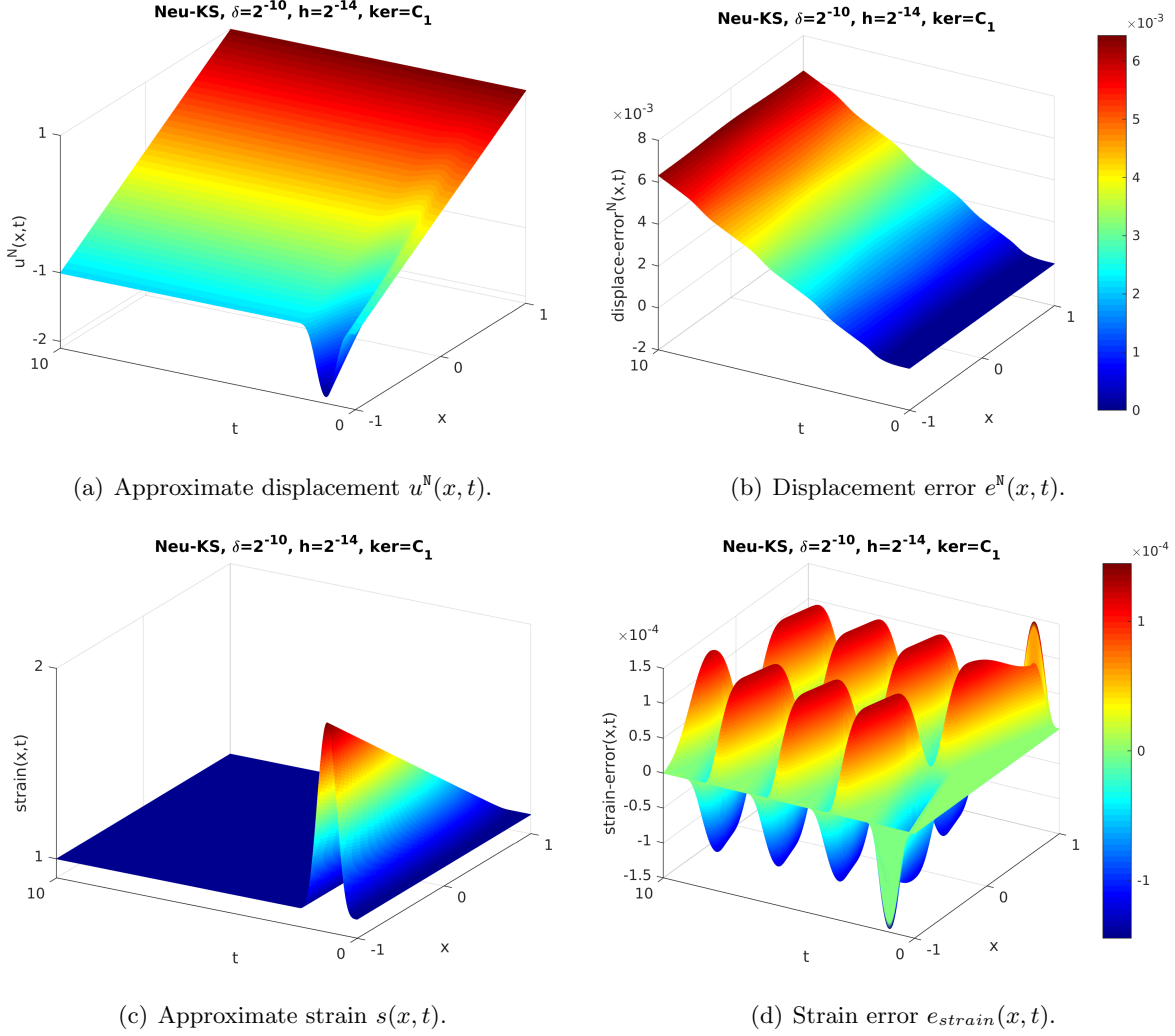


FIGURE 9.3. Displacement of the Neumann problem with known exact solution with $\delta = 2^{-10}$, $h = 2^{-14}$, $\Delta t = 0.50 \times 10^{-3}$, and kernel function $C_1(x)$.

was used, which gave rise to $e^N(x_i, t_j) = e_{\text{strain}}^N(x_i, t_j) = \mathcal{O}(10^{-3}) = \mathcal{O}(\Delta t + h)$; see Fig. 9.2 and Fig. 9.3. The Neumann problem is less accurate and seems more sensitive to grid spacing than the Dirichlet problem.

9.2. Dirichlet and Neumann Problem with Unknown Exact Solution. In this section, we report experiments for the Dirichlet problem (1.1) with unknown exact solution (numerical solution only). We choose zero initial data, i.e., $u^D(x, 0) = u_t^D(x, 0) = 0$, and zero forcing function in the interior so that the wave propagation is initiated only by the boundary data.

The same boundary data are used for both Dirichlet and Neumann problems:

$$\alpha_-^{\text{BC}}(t) := \begin{cases} \frac{1}{4}(1 - \cos(\pi t))^2, & t \in [0, 2] \\ 0, & t \in (2, 10] \end{cases} \quad \text{and} \quad \alpha_+^{\text{BC}}(t) := 0, \quad t \in [0, 10], \quad (9.4)$$

where

$$u^{\text{D}}(\pm 1, t) = \alpha_{\pm}^{\text{D}}(t) \quad \text{and} \quad \frac{\partial u^{\text{N}}}{\partial x}(\pm 1, t) = \alpha_{\pm}^{\text{N}}(t).$$

Reflecting on (3.10)₁ and the interpolation strategy in Sec. 8, more specifically (8.4), for the kernel C_1 the forcing functions respectively become

$$\begin{aligned} b^{\text{D}}(\pm 1, t) &= \frac{d^2 \alpha_{\pm}^{\text{D}}}{dt^2}(t) + \frac{2}{\delta^3} c_1 \alpha_{\pm}^{\text{D}}(t) & \text{and} & \quad b^{\text{D}}(x, t) = 0, \quad x \in \Omega, \\ b^{\text{N}}(\pm 1, t) &= -\frac{\delta}{2} \left(\frac{d^2 \alpha_{\pm}^{\text{N}}}{dt^2}(t) + \frac{2}{\delta^3} c_1 \alpha_{\pm}^{\text{N}}(t) \right) & \text{and} & \quad b^{\text{N}}(x, t) = 0, \quad x \in \Omega. \end{aligned}$$

Wave patterns consisting of multiple reflections of opposite sign can be seen in Fig. 9.4 that are reminiscent of solutions to the classical wave equation. A grid spacing of $h = 2^{-10}$ was chosen. The cases of $\delta = h$ and $\delta = 4h, 16h$ correspond to local and nonlocal computations, respectively. The results for both kernels are shown in Fig. 9.4. The wave speed with kernel function C_2 is slower than that with kernel function C_1 . Furthermore, a larger δ size gives rise to a slower wave speed; see Fig. 9.4.

Using the same BC as in (9.4), a numerical experiment with nonzero initial displacement illustrates wave collision and superposition; see Fig. 9.5. For the kernel C_1 case with $\delta = 2^{-10}$, observe that the reflection of the initial displacement splits the boundary data. For the kernel C_2 case, wave propagation is slower and reflection takes place at a time later than $t = 2$. As a result, reflection does not split the boundary data.

The strain is computed from the displacement data using a central difference approximation. The boundary data for the Neumann problem is chosen to be the same as the Dirichlet problem so that the strain profiles are identical to that of displacement of the Dirichlet problem. One can also rigorously show this equivalence, which we skip here. We simply use the equivalence to verify the validity of numerical experiments with Neumann BC. Note that strain profiles in Fig. 9.6 are identical to displacement profiles in Fig. 9.4. For the strain, a reflection pattern with opposite sign is observed, which agrees with the classical solution. The cascading displacement profile also agrees with that of the classical problem; see Fig. 9.7.

10. CONCLUSION

A comprehensive treatment on how to enforce inhomogeneous local BC in nonlocal problems was presented. We explained methodically how to construct forcing functions to enforce local BC and their relationship to initial values. Exact solutions with both homogeneous and inhomogeneous BC were derived and used to verify numerical experiments. We explained the critical role of the Hilbert-Schmidt property in enforcing local BC rigorously. For the strain BC, an interpolation strategy was prescribed to find the appropriate value of the forcing function from its derivative.

Our ongoing work aims to extend these operators to vector valued problems which will help apply peridynamics to problems that require local BC. Furthermore, construction of higher order node based collocation in higher dimensions is work in progress. Our construction depends on the assumption of a rectangular/box geometry [6]. We are investigating the case of general geometry in higher dimensions.

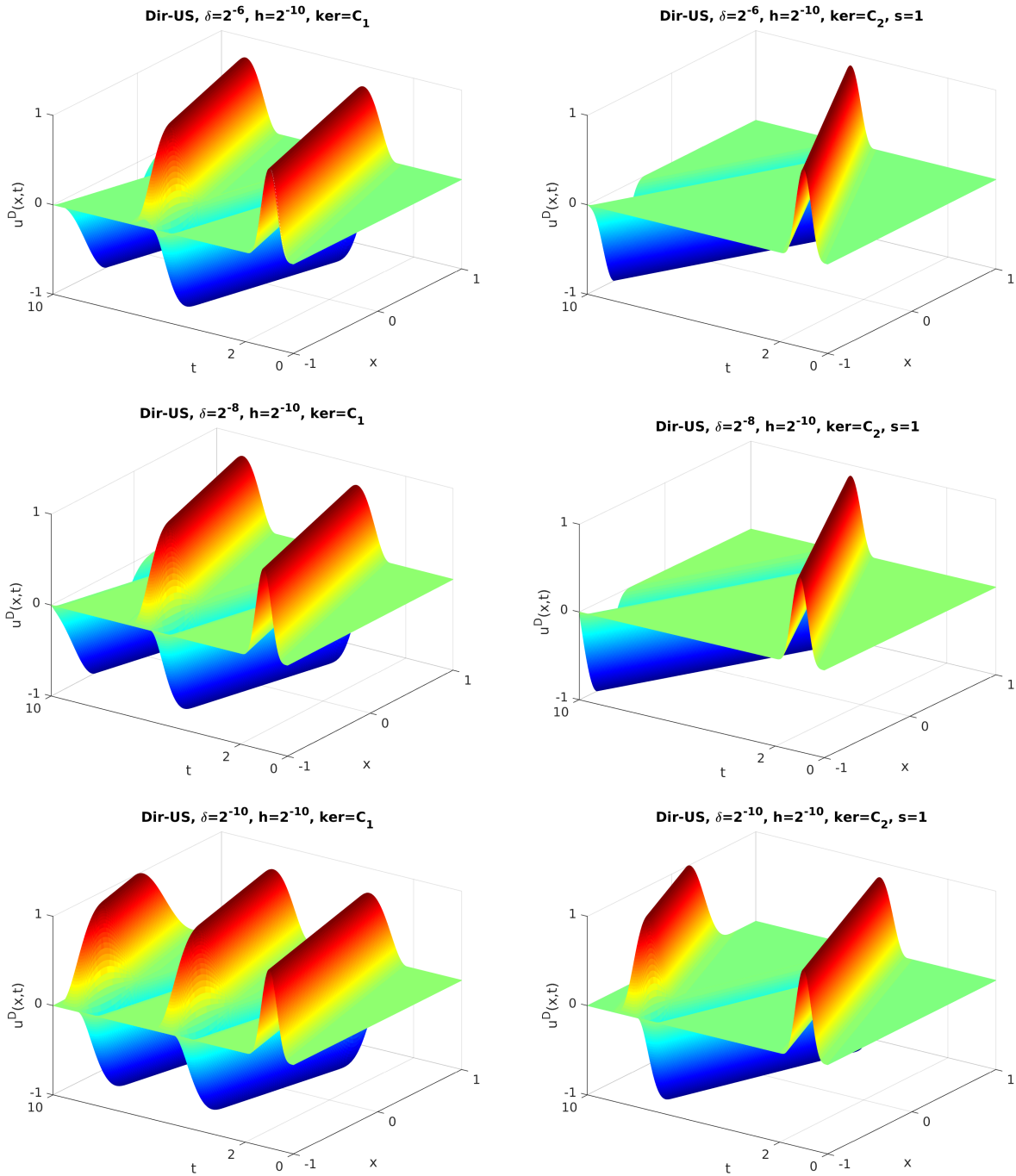


FIGURE 9.4. Approximate displacement $u^D(x,t)$ of the Dirichlet problem with unknown solution with $\delta = 2^{-6}, 2^{-8}, 2^{-10}$, $h = 2^{-10}$, $\Delta t = 0.95 \times 10^{-3}$, and kernel function $C_1(x)$ (left) and $C_2(x)$ and $s = 1$ (right).

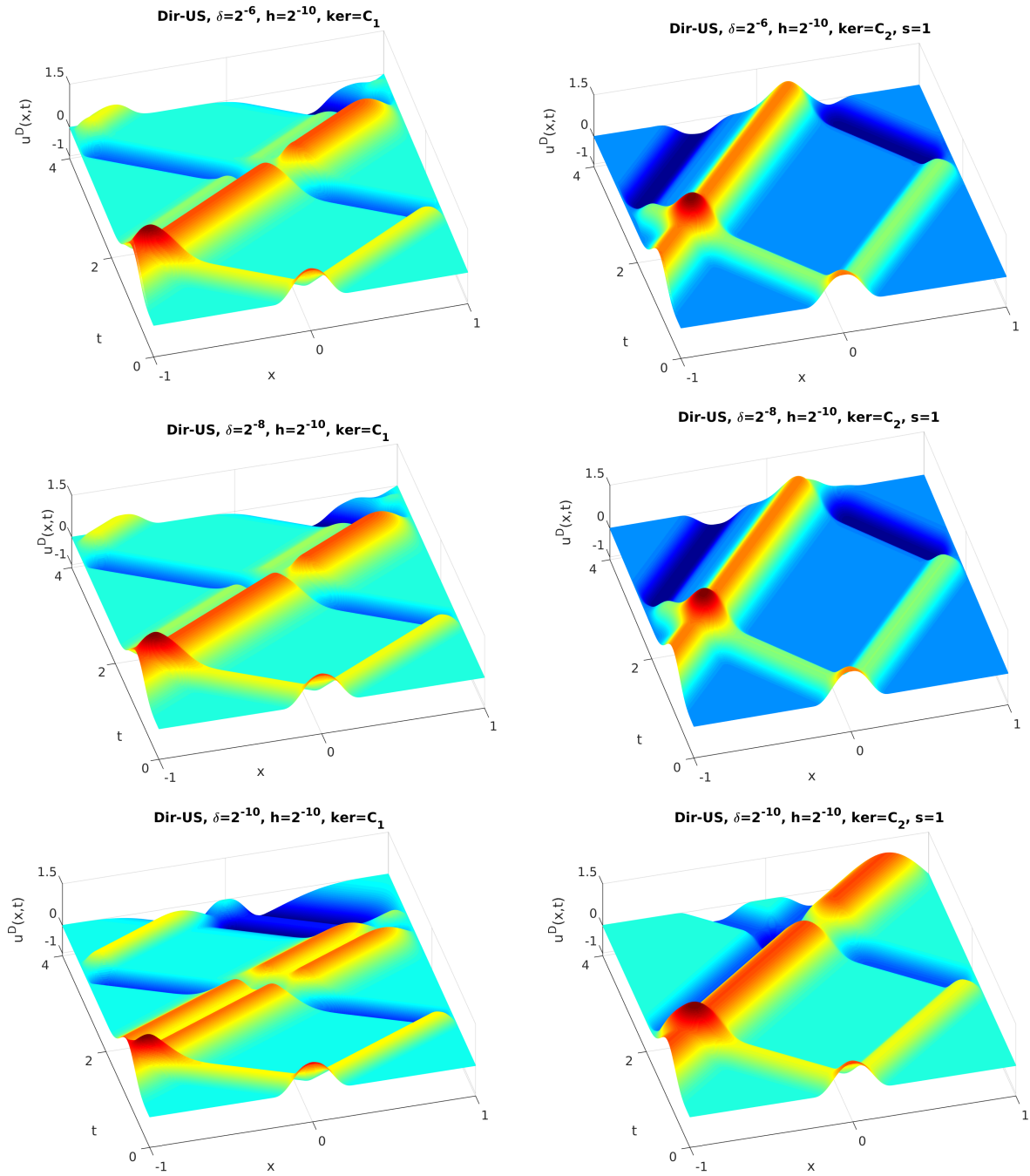


FIGURE 9.5. Approximate displacement $u^D(x,t)$ of the Dirichlet problem with unknown solution with $\delta = 2^{-6}, 2^{-8}, 2^{-10}$, $h = 2^{-10}$, $\Delta t = 0.95 \times 10^{-3}$, kernel function $C_1(x)$ (left) and $C_2(x)$, $s = 1$ (right), and nonzero initial displacement.

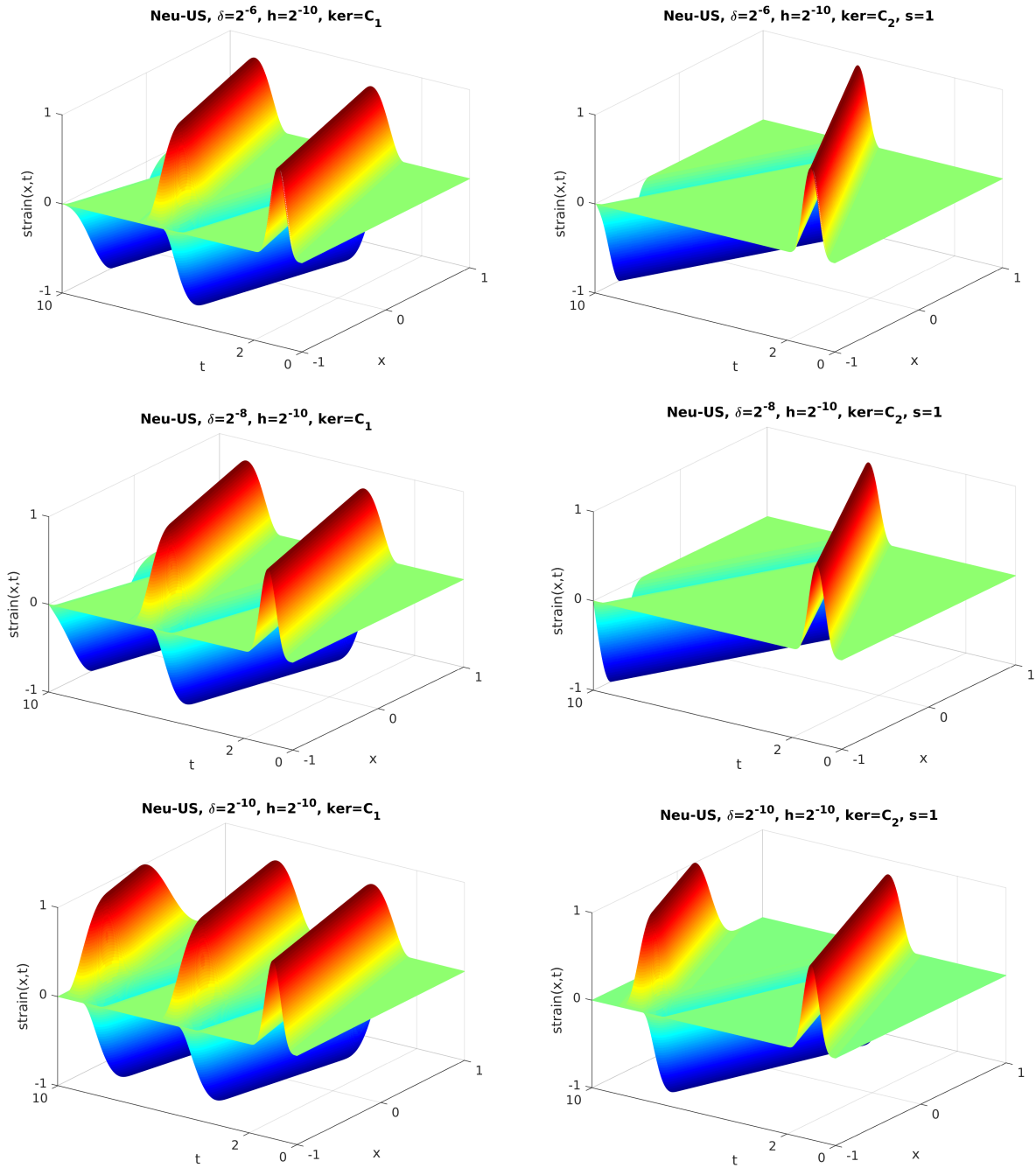


FIGURE 9.6. Approximate strain $s(x,t)$ of the Neumann problem with unknown solution with $\delta = 2^{-6}, 2^{-8}, 2^{-10}$, $h = 2^{-10}$, $\Delta t = 0.95 \times 10^{-3}$, kernel function $C_1(x)$ (left) and $C_2(x)$ and $s = 1$ (right).

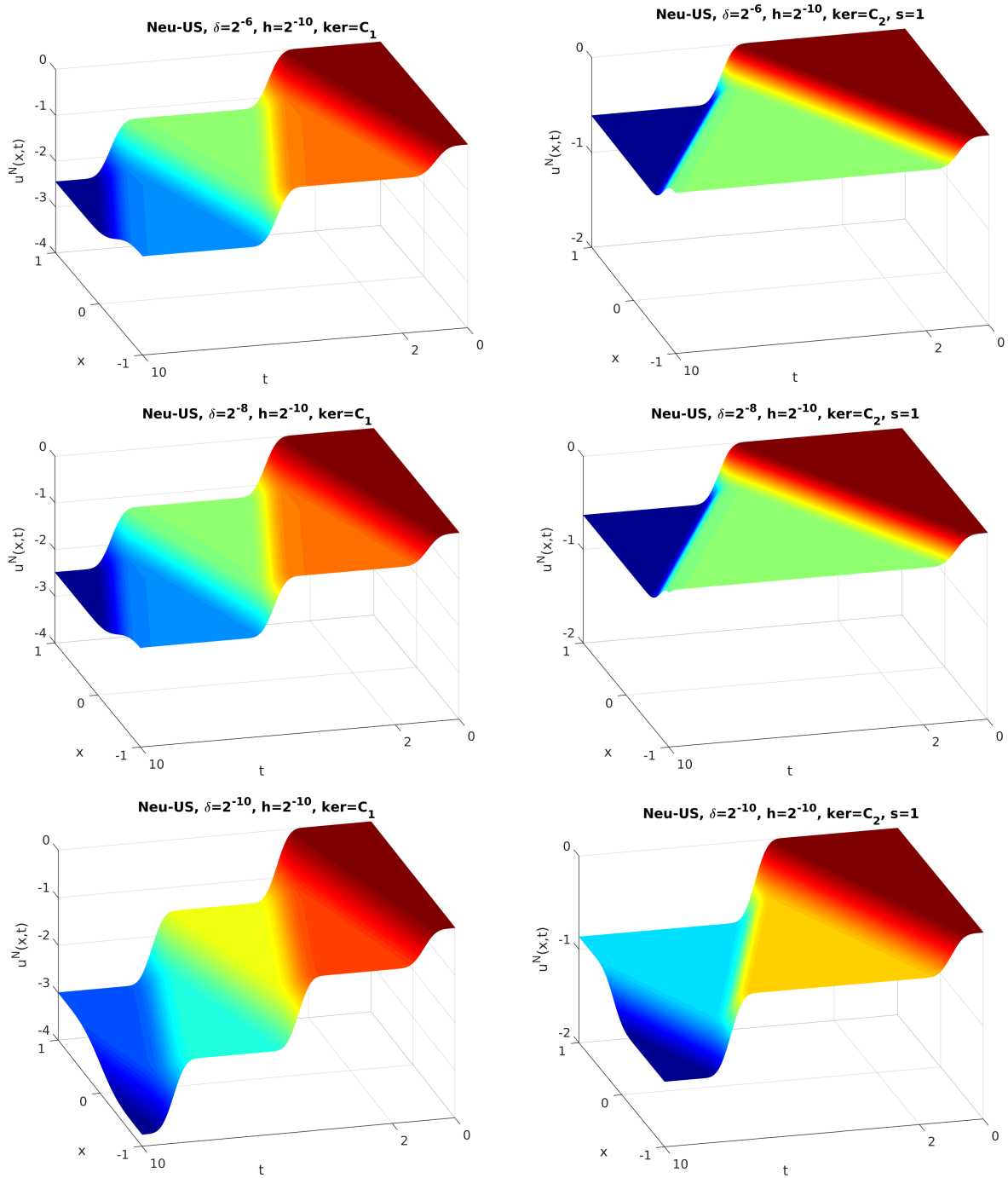


FIGURE 9.7. Approximate displacement $u^N(x, t)$ of the Neumann problem with unknown solution with $\delta = 2^{-6}, 2^{-8}, 2^{-10}$, $h = 2^{-10}$, $\Delta t = 0.95 \times 10^{-3}$, kernel function $C_1(x)$ (left) and $C_2(x)$ and $s = 1$ (right).

Acknowledgment. Research was sponsored by the Army Research Laboratory and was accomplished under Cooperative Agreement Number W911NF-18-2-0090. The views and conclusions contained in this document are those of the authors and should not be interpreted as representing the official policies, either expressed or implied, of the Army Research Laboratory or the U.S. Government. The U.S. Government is authorized to reproduce and distribute reprints for Government purposes notwithstanding any copyright notation herein.

REFERENCES

- [1] Aksoylu, B., Beyer, H.R., Celiker, F.: Application and implementation of incorporating local boundary conditions into nonlocal problems. *Numer. Funct. Anal. Optim.* **38**(9), 1077–1114 (2017). DOI 10.1080/01630563.2017.1320674
- [2] Aksoylu, B., Beyer, H.R., Celiker, F.: Theoretical foundations of incorporating local boundary conditions into nonlocal problems. *Rep. Math. Phys.* **40**(1), 39–71 (2017). DOI 10.1016/S0034-4877(17)30061-7
- [3] Aksoylu, B., Celiker, F.: Comparison of nonlocal operators utilizing perturbation analysis. In: B.K. et al. (ed.), *Numerical Mathematics and Advanced Applications ENUMATH 2015, Lecture Notes in Computational Science and Engineering*, vol. 112, pp. 589–606. Springer (2016). DOI 10.1007/978-3-319-39929-4_57
- [4] Aksoylu, B., Celiker, F.: Nonlocal problems with local Dirichlet and Neumann boundary conditions. *J. Mech. Mater. Struct.* **12**(4), 425–437 (2017). DOI 10.2140/jomms.2017.12.425
- [5] Aksoylu, B., Celiker, F., Kilicer, O.: Nonlocal Operators with Local Boundary Conditions: An Overview, In: G.Z. Voyiadjis (ed.), *Handbook of Nonlocal Continuum Mechanics for Materials and Structures*, (2019), pp. 1293–1330. Springer International Publishing, Cham. DOI 10.1007/978-3-319-58729-5_34
- [6] Aksoylu, B., Celiker, F., Kilicer, O.: Nonlocal problems with local boundary conditions in higher dimensions. *Adv. Comp. Math.* **45**(1), 453–492 (2019). DOI 10.1007/s10444-018-9624-6
- [7] Aksoylu, B., Gazonas, G.A.: Inhomogeneous local boundary conditions in nonlocal problems. In proceedings of ECCOMAS2018, 6th European Conference on Computational Mechanics (ECCM 6) and 7th European Conference on Computational Fluid Dynamics (ECFD 7), 11-15 June 2018, Glasgow, UK. In press.
- [8] Aksoylu, B., Kaya, A.: Conditioning and error analysis of nonlocal problems with local boundary conditions. *J. Comput. Appl. Math.* pp. 1–19 (2018). DOI 10.1016/j.cam.2017.11.023
- [9] Aksoylu, B., Unlu, Z.: Conditioning analysis of nonlocal integral operators in fractional Sobolev spaces. *SIAM J. Numer. Anal.* **52**(2), 653–677 (2014). DOI 10.1137/13092407X
- [10] Beyer, H.R., Aksoylu, B., Celiker, F.: On a class of nonlocal wave equations from applications. *J. Math. Phys.* **57**(6), 062902 (2016). DOI 10.1063/1.4953252. Eid: 062902
- [11] Bitsadze, A.: *Equations of Mathematical Physics*. Mir Publishers, Moscow (1980)
- [12] Du, Q.: An invitation to nonlocal modeling, analysis and computation. In: B. Sirakov, P.N. de Souza, M. Viana (eds.) *Proceedings of the International Congress of Mathematicians 2018 (ICM 2018)*, vol. 3, pp. 3523–3552. World Scientific (2018)
- [13] Du, Q., Gunzburger, M., Lehoucq, R.B., Zhou, K.: Analysis and approximation of nonlocal diffusion problems with volume constraints. *SIAM Rev.* **54**, 667–696 (2012)
- [14] Du, Q., Lipton, R.: *Peridynamics, Fracture, and Nonlocal Continuum Models*. SIAM News, Volume 47, Number 3, April 2014
- [15] Greenberg, M.D.: *Advanced Engineering Mathematics; Second Edition*. Prentice Hall (1998)
- [16] Madenci, E., Oterkus, E.: *Peridynamic Theory and Its Applications*. Springer, New York Heidelberg Dordrecht London (2014). DOI 10.1007/978-1-4614-8465-3
- [17] Silling, S.: Reformulation of elasticity theory for discontinuities and long-range forces. *J. Mech. Phys. Solids* **48**, 175–209 (2000)
- [18] Silling, S., Lehoucq, R.B.: Peridynamic theory of solid mechanics. *Adv. Appl. Mech.* **44**, 73–168 (2010)
- [19] Strauss, W.A.: *Partial Differential Equations: An Introduction*. John Wiley & Sons, Inc., New Jersey, USA (2008)